From:	Jay Borkland
To:	Dierker, Carl; Catri, Cindy; Williams, Ann; Marsh, Michael; LeClair, Jacqueline; Stanley, Elaine; Tisa, Kimberly; Colarusso, Phil; ginny.lombardo@epa.gov
Cc:	bwhite@masscec.com; Hines, Eric; Chet Myers; Gregory Dolan; John McAllister
Subject:	Updated Jasco Report - South Terminal Project
Date:	Wednesday, September 04, 2013 7:25:36 PM
Attachments:	image007.jpg image008.png image009.png P001192 Apex New Bedford Modeling 2012.pdf

---

Hello Carl, et al:

Bill and Eric asked that I forward on to you the updated Jasco Report for your consideration. Please note that the sections that were modified are highlighted in yellow so that you can easily identify the new text. According to Jasco, the remainder of the report has not changed from the previously submitted version. Please feel free to contact us if you have questions.

Thank you. - Jay

Jay Borkland
Apex Companies, LLC
125 Broad Street, 5th Floor
Boston, MA 02110
O) 617-728-0070 x111 M) 617-513-0640

Follow Apex on and Like us on

Privacy Notice: This message and any attachment(s) hereto are intended solely for the individual(s) listed in the masthead. This message may contain information that is privileged or otherwise protected from disclosure. Any review, dissemination or use of this message or its contents by persons other than the addressee(s) is strictly prohibited and may be unlawful. If you have received this message in error, please notify the sender by return e-mail and delete the message from your system. Thank you.

SDMS Doc ID 549032

Underwater Acoustic Modeling of Construction Activities

Marine Commerce South Terminal in New Bedford, MA

Submitted to:
Apex Companies, LCC
125 Broad Street, 5th Floor
Boston, MA 02210

Authors:
Marie-Noël R. Matthews
Mikhail Zykov

4 September 2013

P001192
Document 00420
Version 4.0

JASCO Applied Sciences (Canada) Ltd
2305–4464 Markham Street
Victoria, BC V8Z 7X8 Canada
Tel: +1-250-483-3300
Fax: +1-250-483-3301

Document Version Control

Version	Date	Name	Change
0.1	2012 Oct 03	M-N R Matthews	Initial draft–no results. Released to client for review.
1.0	2012 Oct 26	M-N R Matthews	Draft released to client for review.
2.0	2012 Oct 29	M-N R Matthews	Addressed comments from client. Sent to client.
3.0	2012 Nov 15	M-N R Matthews	Addressed comments from client. Sent to client as final version.
4.0	2013 Sep 03	M-N R Matthews	Significant changes in blast estimation approach from previous version (the sections with major changes were highlighted in yellow). Sent to client.

Suggested citation:

Matthews, M.-N.R. and M. Zykov. 2013. *Underwater Acoustic Modeling of Construction Activities: Marine Commerce South Terminal in New Bedford, MA*. JASCO Document 00420, Version 4.0. Technical report by JASCO Applied Sciences for Apex Companies, LCC.

Contents

1. INTRODUCTION 1
1.1. Fundamentals of Underwater Acoustics 2
1.1.1. Properties of Sound 3
1.1.2. Acoustic Metrics 4
1.1.2.1. Metrics for Continuous Sound 4
1.1.2.2. Metrics for Impulsive Sound 5
1.1.2.3. Metrics for Explosive Sound 7
1.1.3. Source Level and Transmission Loss 7
1.1.4. Spectral Density and 1/3-Octave Band Analysis 7
1.2. Acoustic Impact Criteria 9
2. METHODS 10
2.1. Model Scenarios 10
2.2. Acoustic Source Levels 10
2.2.1. Pile Driving 10
2.2.2. Rock Removal–Non-Explosive 11
2.2.3. Rock Removal–Explosive 11
2.3. Sound Propagation Models 14
2.3.1. Marine Operations Noise Model 14
2.3.2. Cumulative Sound Exposure Levels 15
3. MODEL PARAMETERS 17
3.1. Environmental Parameters 17
3.1.1. Bathymetry 17
3.1.2. Geoacoustics 17
3.1.3. Sound Speed Profile 18
3.2. Geometry and Modeled Volume 19
4. RESULTS 20
4.1. Source Levels 20
4.1.1. Pile Driving 20
4.1.2. Rock Removal–Non-Explosive 21
4.1.3. Rock Removal–Explosive 23
4.2. Sound Fields 24
4.2.1. Pile Driving 25
4.2.2. Rock Removal–Non-Explosive 28
4.2.3. Rock Removal–Explosive 33
LITERATURE CITED 37

Figures

Figure 1. Location of the proposed Marine Commerce Terminal ( ) and the model scenario locations (★) in New Bedford Harbor, MA. 2
Figure 2. Snapshot of the pressure disturbance due to a plane harmonic sound wave. 3
Figure 3. Example waveform showing a continuous noise measurement and the corresponding root-mean-square (rms) sound pressure. 5
Figure 4. Example waveform showing an impulsive noise measurement. Horizontal lines indicate the peak pressure and 90% root-mean-square (rms) pressure for this impulse. The gray area indicates the 90% energy time interval (T_{90}) over which the rms pressure is computed. 6
Figure 5. Example power spectrum of ambient noise and the corresponding 1/3-octave band sound pressure levels. Frequency is plotted on a logarithmic scale, so the 1/3-octave bands are larger at higher frequencies. 8
Figure 6. Diagram of pressure wave paths to a receiver in the water column (not to scale). 13
Figure 7. Peak and root-mean-square (rms) sound pressure level (SPL) and sound exposure level (SEL) versus range from a 20 in^3 airgun array. Solid line is the least squares best fit to rms SPL. Dashed line is the best-fit line increased by 3.0 dB to exceed 90% of all rms SPL values (90th percentile fit) (Ireland et al. 2009, Fig. 10). 15
Figure 8. Sound speed profiles sampled at various locations and times of year within New Bedford Harbor, MA. 19
Figure 9. Estimated 1/3-octave band source level spectra for pile driving operations. 20
Figure 10. Estimated 1/3-octave band source level spectra for cutter-head dredges, clamshell bucket dredges, and a 24-inch hammer drill. 23
Figure 11. Modeled pressure waveform at the seabed, at a distance of 38, 80, and 160 ft from the detonation of a 30-lb charge. 24
Figure 12. Pile driving with a vibratory hammer at Site 2: Received maximum-over-depth root-mean-square (rms) sound pressure levels (SPLs). Blue contours indicate water depth in feet. 26
Figure 13. Pile driving with a vibratory hammer at Site 2: Received maximum-over-depth sound level thresholds. Blue contours indicate water depth in feet. 27
Figure 14. Non-explosive rock removal at Site 1: Received maximum-over-depth root-mean-square (rms) sound pressure levels (SPLs). Blue contours indicate water depth in feet. 29
Figure 15. Non-explosive rock removal at Site 1: Received maximum-over-depth sound level thresholds. Blue contours indicate water depth in feet. 30
Figure 16. Non-explosive rock removal at Site 2: Received maximum-over-depth root-mean-square (rms) sound pressure levels (SPLs). Blue contours indicate water depth in feet. 31
Figure 17. Non-explosive rock removal at Site 2: Received maximum-over-depth sound level thresholds. Blue contours indicate water depth in feet. 32
Figure 18. Explosive charge at Site 2: Peak pressure threshold of 75.6 psi for explosive charges between 30 and 150 lbs. Blue contours indicate water depth in feet. 35
Figure 19. Explosive charge at Site 2: Impulse level threshold of 18.4 psi·msec for explosive charges between 30 and 150 lbs. Blue contours indicate water depth in feet. 36

Tables

Table 1. The nominal center frequencies of 1/3-octave bands, from 10 Hz to 20 kHz..... 9
Table 2. List of model scenarios. Site 2 is located at the north edge of proposed South Terminal. Site 1 is located within the northern section of the South Terminal dredge footprint (Figure 1). 10
Table 3. Estimated geoacoustic profile for Sites 1 and 2. Within each sediment layer, parameters vary linearly within the stated range..... 18
Table 4. Estimated geoacoustic parameter for grey granite bedrock (gneiss) found in Dredge areas 2 and 3 (Figure 1). 18
Table 5. Dredges Specifications..... 22
Table 6. Distances to peak pressure injury criterion of 75.6 psi. 34
Table 7. Distances to impulse injury criterion of 18.4 psi-msec..... 34

1. Introduction

Construction of the proposed Marine Commerce Terminal (South Terminal) in New Bedford, MA, will require pile driving, non-explosive rock removal, and (possibly) explosive rock removal. This report presents the results of an underwater acoustic modeling study of the proposed construction site. JASCO Applied Sciences (JASCO) carried out this study for Apex Companies, LCC (Apex) in support of the construction project's biological assessment for the Atlantic sturgeon (*Acipenser oxyrinchus*). Interpretation of potential effects of noise on marine life, including Atlantic sturgeon, is outside the scope of this report.

The model scenarios were chosen to evaluate precautionary distances to threshold levels for each construction activity, at the time of year when the water conditions allow sound to propagate the farthest from the source. Five scenarios were modeled:

- One pile driving scenario at Site 2, along the extended South Terminal bulkhead,
- Two non-explosive rock removal scenarios at Sites 1 and 2, within South Terminal dredge footprint, and
- One explosive rock removal scenario at Site 2 (Figure 1).

The sound levels estimated from this study are presented in two formats: as contour maps of the sound fields that show the directivity and range to various sound level thresholds and as maximum and 95% distances to some sound level thresholds. The distances from the sound sources to sound level thresholds, representing pile driving and non-explosive rock removal operations, are provided for:

- Peak sound pressure level (SPL) of 206 dB re 1 µPa,
- Cumulative sound exposure level (cSEL) of 187 dB re 1 $\mu Pa^2 \cdot s$,
- root-mean-square (rms) SPL from 200 to 120 dB re 1 µPa in 10 dB steps, and
- Sound exposure level (SEL) from 200 to 120 dB re 1 µPa in 10 dB steps (for impulse sound sources only).

The distances to sound level thresholds for the use of explosives are provided for:

- Peak pressure of 75.6 psi, and
- Impulse level of 18.4 psi-msec.

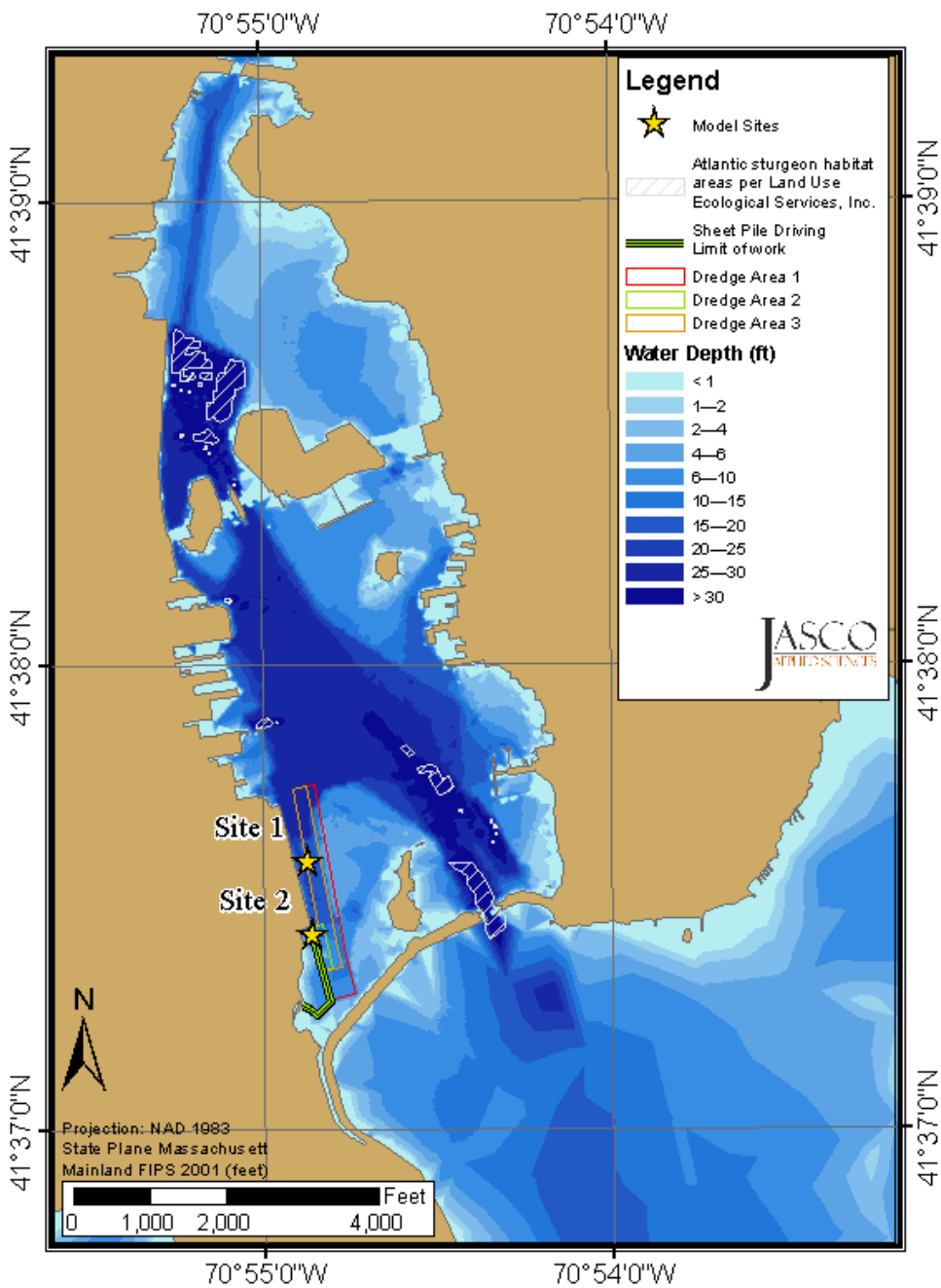

Figure 1. Location of the proposed Marine Commerce Terminal ( ) and the model scenario locations ( ) in New Bedford Harbor, MA.

1.1. Fundamentals of Underwater Acoustics

Sound is the result of mechanical vibration waves traveling through a fluid medium such as air or water. These vibration waves generate a time-varying pressure disturbance that oscillates above and below the ambient pressure. Sound waves may be perceived by the auditory system of an animal, or they may be measured with an acoustic sensor (a microphone or hydrophone). Water conducts sound over four times faster than air due to its lower compressibility; the speed of sound travelling in water is roughly 4900 ft/s, compared to 1100 ft/s in air. Sound is used

extensively by marine organisms for communication and for sensing their environment. Humans may use sound purposely to probe the marine environment through technologies like sonar; more often, human activities such as marine construction produce underwater sound as an unintended side effect.

Sources of underwater sound can be mechanical (e.g., a ship), biological (e.g., a whale) or environmental (e.g., rain). *Noise*, in general parlance, refers to unwanted sound that may affect humans or animals. Noise at relatively low levels can form a background that interferes with the detection of other sounds; at higher levels, noise can also be disruptive or harmful. Common sources of naturally occurring underwater environmental noise include wind, rain, waves, seismic disturbances, and vocalizations of marine fauna. Anthropogenic (i.e., manmade) sources of underwater noise include marine transportation, construction, geophysical surveys, and sonar. Underwater noise usually varies with time and location.

1.1.1. Properties of Sound

The fundamental properties of sound waves are amplitude, frequency, wavelength, and intensity. Frequency of a sound wave, f, is the rate of pressure oscillation per unit of time. Amplitude of a sound wave, A, is the maximum absolute pressure deviation of the wave. If c is the speed of sound in a medium, then the pressure disturbance, P, due to a plane harmonic sound wave (Figure 2) at time t and location x is:

$$P(x,t) = A\cos(2\pi f(x/c - t)) \tag{1}$$

The wavelength, λ, is the distance traveled by a sound wave over one complete cycle of oscillation. For plane harmonic sound waves, the wavelength is equal to the frequency divided by the speed of sound:

$$\lambda = \frac{f}{c} \tag{2}$$

Harmonic waves are fundamentally in acoustics because a well-known mathematical law (Fourier's theorem) states that any arbitrary waveform can be represented by the superposition of harmonic waves.

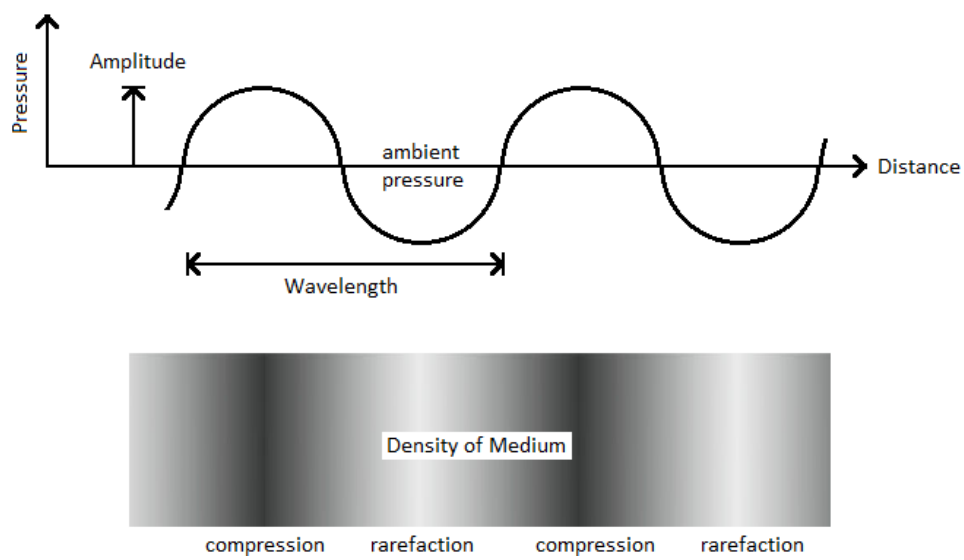

Figure 2. Snapshot of the pressure disturbance due to a plane harmonic sound wave.

The intensity of a traveling sound wave is the acoustic power per unit area carried by the wave. In general, the intensity of a sound wave is related to the wave's amplitude, but it also depends on the compressibility and density of the acoustic medium. The loudness of a sound is related to the intensity; however, loudness is a subjective term that refers to the *perception* of sound intensity, rather than to the actual intensity itself. For humans and other animals, perceived loudness also depends on the frequency and duration of the sound.

1.1.2. Acoustic Metrics

Sound pressure and intensity are commonly measured on the decibel (dB) scale. The decibel scale is a logarithmic scale that expresses a quantity relative to a predefined reference quantity. Sound pressure in decibels is expressed in terms of the sound pressure level (SPL, symbol L_p):

$$L_p = 20\log_{10}\left(P / P_{ref}\right) \tag{3}$$

where P is the pressure amplitude and P_{ref} is the reference sound pressure. For underwater sound, the reference pressure is 1 µPa (i.e., 10^{-6} Pa or 10^{-11} bar). In most cases, sound intensity is directly proportional to the mean square of the sound pressure (i.e., $I \propto \langle P^2 \rangle$); therefore, SPL is considered synonymous with sound intensity level.

The decibel scale for measuring underwater sound is different than for measuring airborne sound. Airborne decibels are based on a standard reference pressure of 20 µPa, which is 20 times greater than the hydroacoustic reference pressure of 1 µPa. Furthermore, due to differences in compressibility and density between the two media, the impedance relationship between sound pressure and sound intensity is different in air than in water. Accounting for these differences in reference pressure and acoustic impedance, for a sound wave with the same intensity in both media, the hydroacoustic decibel value (in dB re 1 µPa) is about 63 dB greater than the airborne decibel value (in dB re 20 µPa).

Sounds that are composed of single frequencies are called "tones." Most sounds are generally composed of a broad range of frequencies ("broadband" sound) rather than pure tones. Sounds with very short durations (less than a few seconds) are referred to as "impulsive." Such sounds typically have a rapid onset and decay. Steady sounds that vary in intensity only slowly with time, or that do not vary at all, are referred to as "continuous."

1.1.2.1. Metrics for Continuous Sound

Continuous sound is characterized by gradual intensity variations over time, e.g., the propeller noise from a transiting ship. The intensity of continuous noise is generally given in terms of the root-mean-square (rms) SPL. Given a measurement of the time varying sound pressure, $p(t)$, for a given noise source, the rms SPL (symbol L_p) is computed according to the following formula:

$$L_p = 10\log_{10}\frac{1}{T}\int_T p(t)^2\,dt / P_{ref}{}^2 \tag{4}$$

In this formula, T is time over which the measurement was obtained. Figure 3 shows an example of a continuous sound pressure waveform and the corresponding rms sound pressure.

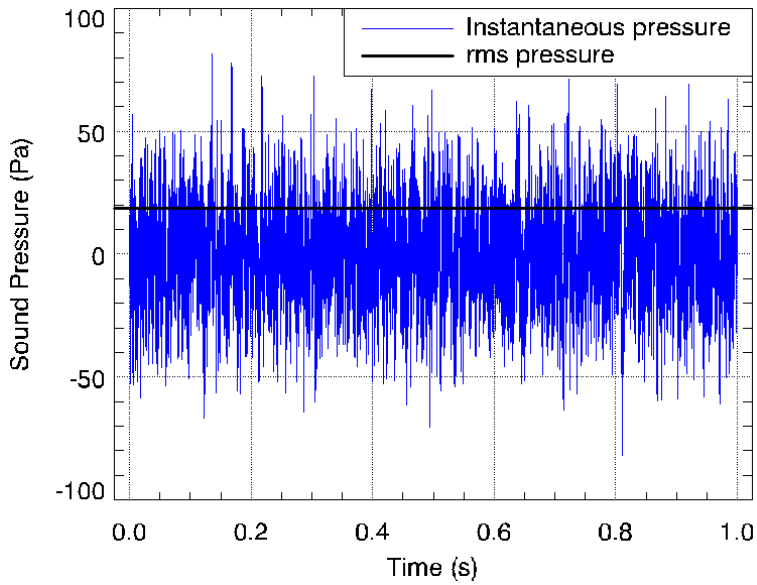

Figure 3. Example waveform showing a continuous noise measurement and the corresponding root-mean-square (rms) sound pressure.

1.1.2.2. Metrics for Impulsive Sound

Impulsive, or transient, sound is characterized by brief, intermittent acoustic events with rapid onset and decay back to pre-existing levels (within a few seconds), e.g., noise from impact pile driving. Impulse sound levels are commonly characterized using three different acoustic metrics: peak pressure, rms pressure, and sound exposure. The peak SPL (symbol L_{pk}) is the maximum instantaneous sound pressure level measured over the impulse duration:

$$L_{\mathrm{pk}} = 20\log_{10}\left(\max\left|p(t)\right| / P_{ref}\right) \tag{5}$$

In this formula, $p(t)$ is the instantaneous sound pressure as a function of time, measured over the impulse duration $0 \le t \le T$. This metric is very commonly quoted for impulsive sounds but does not take into account the duration or bandwidth of the noise.

The rms SPL may be measured over the impulse duration according to the following equation:

$$L_p = 10\log_{10}\left(\frac{1}{T}\int_T p(t)^2\,dt / P_{ref}^2\right) \tag{6}$$

Some ambiguity remains in how the duration T is defined, because in practice the beginning and end of an impulse can be difficult to identify precisely. In studies of impulsive noise, T is often taken to be the interval over which the cumulative energy curve rises from 5% to 95% of the total energy. This interval contains 90% of the total energy (T_{90}), and the SPL computed over this interval is commonly referred to as the 90% rms SPL (L_{p90}). The relative energy, $E(t)$, of the impulse is computed from the time integral of the square pressure:

$$E(t) = \int_0^t p(\tau)^2\,d\tau / P_{ref}^2 \tag{7}$$

According to this definition, if the time corresponding to n% of the total relative energy of the impulse is denoted t_n, then the 90% energy window is defined such that $T_{90} = t_{95}\text{–}t_5$. Figure 4 shows an example of an impulsive sound pressure waveform, with the corresponding peak pressure, rms pressure, and 90% energy time interval.

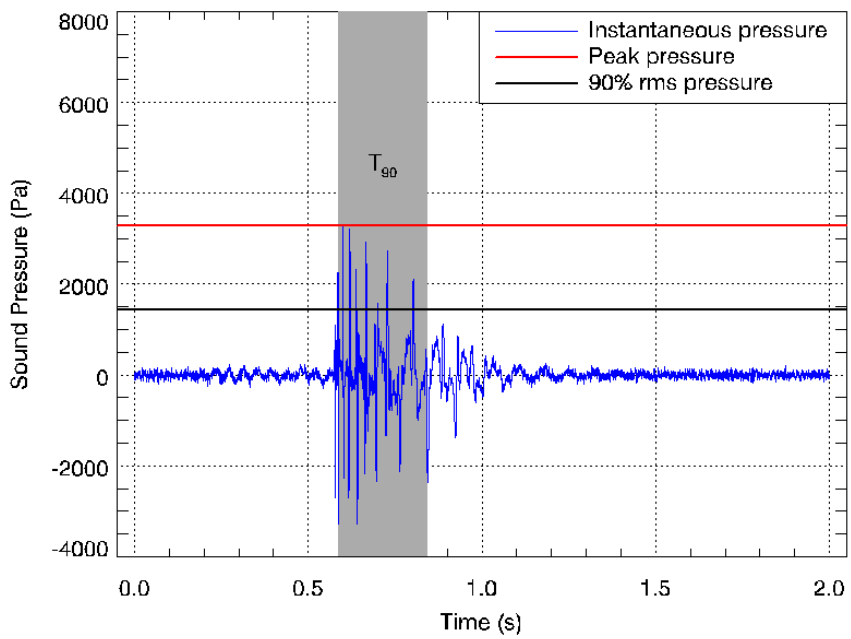

Figure 4. Example waveform showing an impulsive noise measurement. Horizontal lines indicate the peak pressure and 90% root-mean-square (rms) pressure for this impulse. The gray area indicates the 90% energy time interval (T_{90}) over which the rms pressure is computed.

The sound exposure level (SEL, symbol L_E) is a measure of the total sound energy contained in one or more impulses. The SEL for a single impulse is computed from the time-integral of the squared pressure over the impulse duration:

$$L_E = 10\log_{10}\left(\int_{T_{100}} p(t)^2\,dt / P_{ref}^2\right) = 10\log_{10}\left(E\left(T_{100}\right)\right) \tag{8}$$

Unlike SPL, the SEL is generally applied as a dosage metric, meaning that its value increases with the number of exposure events. The cumulative SEL (cSEL) for multiple impulses (symbol $L_E^{(\Sigma)}$) is computed from the linear sum of the SEL values:

$$L_E^{(\Sigma)} = 10\log_{10}\left(\sum_{n=1}^{N} 10^{L_E^{(n)}/10}\right) \tag{9}$$

where N is the total number of impulses, and $L_E^{(n)}$ is the SEL of the nth impulse event. Alternatively, given the mean (or expected) SEL for single impulse events, $\langle L_E \rangle$, the cumulative SEL from N impulses may be computed according the following formula:

$$L_E^{(\Sigma)} = \langle L_E \rangle + 10\log_{10}(N) \tag{10}$$

Sound levels for impulsive noise sources (i.e., impact hammer pile driving) presented in this report refer to single pulse. Because the 90% rms SPL and SEL for a single impulse are both computed from the integral of square pressure, these metrics are related by a simple expression that depends only on the duration of the 90% energy time window T_{90}:

$$L_E = L_{p90} + 10\log_{10}(T_{90}) + 0.458 \tag{11}$$

In this formula, the 0.458 dB factor accounts for the remaining 10% of the impulse energy that is excluded from the 90% time window.

1.1.2.3. Metrics for Explosive Sound

Underwater sound from explosions is most commonly characterized using peak pressure levels (psi), impulse levels (pis·s), or maximum particle velocity (ft/s). In the present report, results are presented in terms of peak pressure and impulse, to conform to the criteria suggested by the National Marine Fisheries Service (Section 1.2).

The peak pressure level is the maximum instantaneous sound pressure level measured over the length of the waveform resulting from an explosion:

$$P_{\mathrm{pk}} = \max\left|p(t)\right| \tag{12}$$

Where $p(t)$ is the instantaneous sound pressure as a function of time.

The impulse is the time integral of pressure through the largest positive phase of a pressure waveform (CSA 2004):

$$I = \int_0^{\tau} p(t)dt \tag{13}$$

In this formula, τ is the end time of the largest positive phase of the pressure waveform. The impulse has units of pounds per square-inch-seconds (psi·s) or pounds per square-inch-milliseconds (psi·msec).

1.1.3. Source Level and Transmission Loss

Sources of underwater noise generate radiating sound waves whose intensity generally decays with distance from the source. The dB reduction in sound level that results from propagation of sound away from an acoustic source is called propagation loss or transmission loss (TL). The loudness or intensity of a noise source is quantified in terms of the source level (SL), which is the sound level referenced to some fixed distance from a noise source. The standard reference distance for underwater sound is 1 m. By convention, transmission loss is quoted in units of dB re 1 m and underwater acoustic source levels are specified in units of dB re 1 μPa at 1 m. In the source-path-receiver model of sound propagation, the received sound level RL at some receiver position **r** is equal to the source level minus the transmission loss along the propagation path between the source and the receiver:

$$\mathrm{RL}(\mathbf{r}) = \mathrm{SL} - \mathrm{TL}(\mathbf{r}) \tag{14}$$

1.1.4. Spectral Density and 1/3-Octave Band Analysis

The discussion of noise measurement presented so far has not addressed the issue of frequency dependence. The sound power per unit frequency of an acoustic signal is described by the power spectral density (PSD) function. The PSD for an acoustic signal is normally computed via the Discrete Fourier Transform (DFT) of time-sampled pressure data. The units of PSD are 1 μPa^2/Hz or dB re 1 μPa^2/Hz. For practical quantitative spectral analysis, a coarser representation of the sound power distribution is often better suited. In 1/3-octave band analysis, an acoustic signal is filtered into multiple, non-overlapping passbands before computing the SPL. These 1/3-octave bands are defined so that three adjacent bands span approximately one octave

(i.e., a doubling) of frequency. Figure 5 shows an example of power spectral density levels and corresponding 1/3-octave band pressure levels for an ambient noise recording.

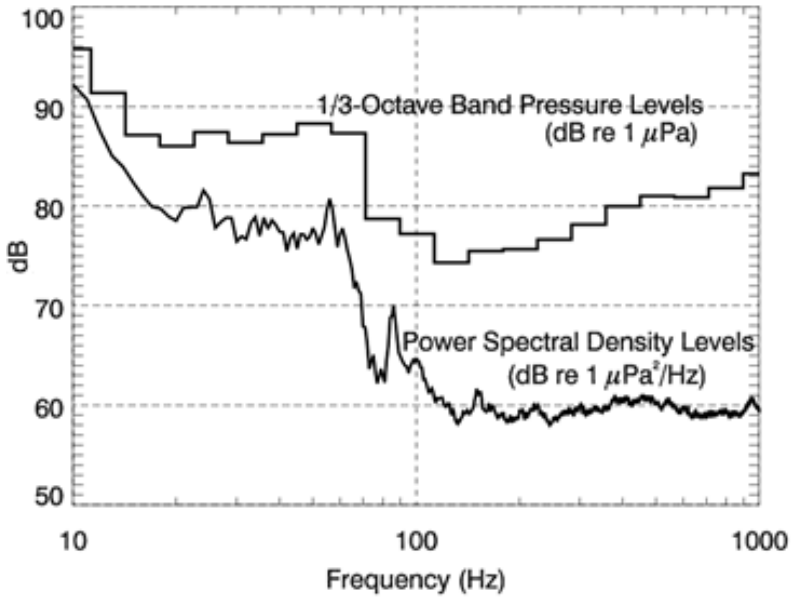

Figure 5. Example power spectrum of ambient noise and the corresponding 1/3-octave band sound pressure levels. Frequency is plotted on a logarithmic scale, so the 1/3-octave bands are larger at higher frequencies.

Standard center frequencies, f_c, for 1/3-octave passbands are given by:

$$f_c(n) = 10^{n/10} \quad n = 1, 2, 3... \tag{15}$$

Nominal 1/3-octave band center frequencies, according to ISO standards, for the range relevant to this study are listed in Table 1. The SPL inside a 1/3-octave band, $L_{pb}(f_c)$, is related to the average PSD level inside that frequency band, $L_{ps}^{(avg)}(f_c)$, by the bandwidth, Δf:

$$L_{ps}^{(avg)}(f_c) = L_{pb}(f_c) - 10\log_{10}(\Delta f) \tag{16}$$

The bandwidth of a 1/3-octave band is equal to 23.1% of the band center frequency (i.e., $\Delta f = 0.231 f_c$). Spectrum density levels and band levels are not limited to measurements of sound pressure: they may also, with appropriate selection of reference units, be given for SEL.

Table 1. The nominal center frequencies of 1/3-octave bands, from 10 Hz to 20 kHz.

Band Number	Center Frequency (Hz)	Band Number	Center Frequency (Hz)	Band Number	Center Frequency (Hz)	Band Number	Center Frequency (Hz)
10	10	20	100	30	1,000	40	10,000
11	12.5	21	125	31	1,250	41	12,500
12	16	22	160	32	1,600	42	16,000
13	20	23	200	33	2,000	43	20,000
14	25	24	250	34	2,500		
15	31.5	25	315	35	3,150		
16	40	26	400	36	4,000		
17	50	27	500	37	5,000		
18	63	28	630	38	6,300		
19	80	29	800	39	8,000		

1.2. Acoustic Impact Criteria

The acoustic impact criteria considered in this report were based on the recommendation from the National Marine Fisheries Service (NMFS). Currently, NMFS has no formal criteria for assessment of injury, mortality, or behavioral effect on fish created by continuous sound; however, NMFS, through correspondence with Apex, requested that the same impact criteria for impact pile driving (i.e., for impulsive sound) be considered for vibratory pile driving and non-explosive rock removal (i.e., for continuous sound). NMFS uses dual criteria for assessment of injury to finfish by impact hammer pile driving. These criteria, derived from the agreement by the Fisheries Hydroacoustic Working Group (FHWG 2008), are:

- Peak SPLs ≥ 206 dB re 1 µPa or cSELs ≥ 187 dB re 1 $\mu Pa^2 \cdot s$ over 24 hours are estimated to create injury or mortality to fish, and
- rms SPLs ≥ 150 dB re 1 µPa are estimated to have behavioral effects on fish.

By convention, SELs for continuous sources are considered over a 1 s interval, thus are equal to rms SPLs (see Section 1.1.2); therefore, distances to the injury or mortality threshold of 187 dB re 1 $\mu Pa^2 \cdot s$ (cSEL over 24 hours) may be greater than that of behavioral effects threshold on fish (rms SPL of ≥ 150 dB re 1 µPa). Although these criteria are unusual for a continuous source[1], these were the only criteria considered in this report.

Currently, NMFS has no formal criteria for assessment of hydroacoustic impacts of underwater explosion on finfish. The peak pressure levels of ≤ 75.6 psi and impulse levels of ≤ 18.4 psi-msec were previously reported to create no injury or mortality to fish (Bullard 2012, Mosher 1999). These levels were therefore used as impact criteria in this report.

[1] The cSEL criteria for nonpulse (continuous) sound are generally much higher than for impulsive sound (by 17 dB for marine mammals; Southall 2007).

2. Methods

2.1. Model Scenarios

Five scenarios were modeled (Figure 1, Table 2):

- one pile-driving scenario,
- two non-explosive rock removal scenarios, and
- one explosive rock removal scenario.

The model scenarios evaluate precautionary distances to sound level thresholds at the time of year when the water conditions allow the sound to propagate the farthest from the source. For comparison purpose, each type of operation was modeled at Site 2 (northern edge of the proposed terminal; Figure 1). Non-explosive rock removal operations were also modeled at Site 1 (within the northern section of the South Terminal dredge footprint; Figure 1).

Table 2. List of model scenarios. Site 2 is located at the north edge of proposed South Terminal. Site 1 is located within the northern section of the South Terminal dredge footprint (Figure 1).

Scenario	Sound Source	Location
Pile Driving		
1	Vibratory hammer	Site 2
Non-Explosive Rock Removal		
2	Cutter-head dredge	Site 1
3	Cutter-head dredge	Site 2
Explosive Rock Removal		
4	Explosive charges (30 to 150 lbs)	Site 2

2.2. Acoustic Source Levels

2.2.1. Pile Driving

Documentation provided by Apex specified that sheet piles (type AS-500-12.7 (20 inch) or AZ-14-700 (28 inch)) will be driven to form the bulkhead of the proposed South Terminal. Later, 24–36 inch diameter steel piles will be set into pre-drilled holes in front of the sheet pile. The piles will be driven using a vibratory system; however, the exact drilling equipment was undecided at the time of this study.

The energy required to drive a pile depends on the pile size and the soil resistance encountered; therefore, the noise from the pile driving operations is expected to vary throughout the operation. At first, the pile penetration will be shallow and there will be little soil resistance. At the final stage, when the pile penetration approaches the projected depth, the resistance will be strongest and higher energy is needed to drive the pile. The maximum noise levels from the pile driving are expected at the latest stage of driving for each individual pile (Betke 2008).

Measurements of underwater sound levels reported by Illingworth & Rodkin (2007) were used to estimate sound levels from vibratory hammer on 24-inch sheet piles. Review and analysis of past measurements is currently the best available method for estimating source levels for use in predictive models of pile driving. Technical guidelines generally advocate estimating piling source levels from past measurements (CALTRANS 2009, §4.6.2, WSDOT 2010b, §7.2.4). JASCO has applied this method to several projects to predict the underwater noise from pile driving activities (Gaboury et al. 2007a, 2007b, Austin et al. 2009, Erbe 2009, MacGillivray et al 2011).

The reported levels were back-propagated to a reference distance of 3.28 ft (1 m) from the source assuming spherical spreading loss ($20\log R$) up to a distance equal to the water depth and cylindrical spreading loss ($10\log R$) thereafter (where R [m] is the range from the source).

2.2.2. Rock Removal–Non-Explosive

A mechanical or hydraulic type dredge with an enclosed bucket will remove surficial sediment within the South Terminal dredge footprint (dredge areas 1–3 in Figure 1). If the rock is too hard for removal with conventional dredges, different non-explosive rock removal techniques may be used, including:

- Hydraulic impact hammering (Hoe Ram),
- Drilling and fracturing of rock,
- Use of large backhoe, and
- Use of a cutter-head.

The exact specification of the non-explosive rock removal equipment was unknown at the time of this study; thus, the estimated source levels from the different activities considered were compared and the “loudest” technique was modeled to present precautionary estimates of radii to level thresholds.

2.2.3. Rock Removal–Explosive

If non-explosive rock removal methods do not allow for dredging to reach the desired water depth, explosives may be used to fragment the bedrock and facilitate dredging. The blasting of shallow bedrock is expected to occur in dredge areas 2 and 3 (Figure 1). The August 2013 Operational Blasting Plan presents the following characteristics for the proposed blast:

- A blast will consist of a series of about 40 detonations.
- The charges will consist of Blastex Plus TX (Dyno Nobel Inc.).
- The charge weights per delay will range between 38 and 136 lb.
- The minimum spacing between charges will be 8 ft.
- The minimum delay between detonations will be 25 ms.
- The charge diameter will vary between 3.75 and 5.5 in, with a typical diameter of 4.25 in.
- Boreholes will be drilled to depths of 7–22.8 ft, depending on the area, with a subdrill (depth below the contract elevation) of 6 ft, and a minimum of 24 in of crushed stones to cap the blast hole.

- The charges will be detonated offshore to inshore.

Previous versions of this report included results for rock removal using explosives where a 12 dB attenuation factor was applied to model the use of a bubble curtain as mitigation system. This attenuation was shown to apply to charges detonated in water or on the seabed (Nützel 2008). Given that the updated modeling methodology leads to significantly shorter distances to injury thresholds than previously estimated, the present modeling study does not include estimates of the effect of bubble curtain mitigation.

In earlier versions of this report, the specifications of the blast were unknown. The peak pressure and impulse of the pressure waveform were predicted with the UnderWater Calculator spreadsheet developed by Dzwilewski and Fenton (2003), which was designed to predict the acoustic impact of pile removal operations that involved placing a charge inside a pipe pile. The Calculator employs empirical equations for the peak pressure (Ppk, in psi) and the impulse (I, in psi-msec; Swisdak 1978) from a blast:

$$P_{\mathrm{pk}}(r) = 145.0\, K_P \left(\frac{W^{1/3}}{r} \right)^{\alpha_P} \tag{17}$$

$$I(r) = 145.0\, W^{1/3} K_I \left(\frac{W^{1/3}}{r} \right)^{\alpha_I} \tag{18}$$

where W is the effective weight of the explosive charge (in kilograms), r is the slant range from the blast (in meters), and KP, KI, αP, and αI are coefficients specific to a given explosive. These equations were developed for a blast detonated in the water column.

To simulate the shockwave from a charge buried in the sediment, the effective weight of the charge must be adjusted. The kinetic energy coupled into the water is reduced because a portion of the blast energy is absorbed by non-elastic deformations of the sediment. Dzwilewski and Fenton (2003) performed several numerical model runs with the Eulerian hydrocode CTH, a three-dimensional shock wave physics code (McGlaun et al. 1990), to quantify the explosive coupling efficiency for a charge buried in compact clay sediments and for a charge placed inside a steel pipe driven into clay sediments. The coupling efficiency for a 50-lbs C-4 charge in stiff clay sediments was estimated at 79%. The same charge placed inside a 36-inch diameter pile with 1.5-inch wall thickness in clay had 39% coupling efficiency (Dzwilewski and Fenton 2003). The coupling efficiency increased with the charge size. Original results for blast of buried charges at Site 2 (presented in version 3.0 of this report) used charge effective weights for a 24-inch diameter pile with 1-inch wall thickness in stiff clay. However, depending on the type of substrate material, capping material, charge weight, and burial depth, the effect of a blast in the substrate may be as low as 1.4% of a blast in open water (USACE 1999).

Based on the blast specification in the August 2013 Operational Blasting Plan, the peak pressure and impulse in the water column were predicted with the Conventional Weapons Effects (ConWep) software (Hyde 1988, 1992), in conjunction with the UnderWater Calculator spreadsheet (Dzwilewski and Fenton 2003). ConWep allows a more accurate estimate of the shock wave in the substrate and at the seabed. The charge effective weights in the UnderWater Calculator spreadsheet were adjusted based on ConWep results to provide more accurate, yet conservative estimates of distances to peak pressure and impulse criteria.

ConWep uses a set of empirical equations and curves representing the effect from several conventional explosive weapons, including explosives detonated in ground and bedrock, collected by the U.S. Army Corps of Engineers and recorded in the U.S. Army manual TM 5-855-1, Fundamentals of Protective Design for Conventional Weapons. It includes a database of the yield and detonation rates for a number of explosive compounds, including ANFO (Ammonium Nitrate/ Fuel Oil). In ground shock mode, ConWep predicts the peak pressure and impulse at a chosen target range and depth in the substrate (bedrock). The input parameters include the type of explosive, the charge weight, the geometry of the detonation (depth of the charge, distance to the receiver, and depth of the receiver), and the geoacoustic parameters of the substrate (density, compressional-wave (or P-wave) velocity, and attenuation coefficient).

A pressure wave propagating in the substrate will be partially transmitted to the water through the seabed (Figure 6). The ratio of amplitude of the transmitted wave to the incident wave, denoted as the transfer coefficient (T), was calculated based on the impedance values for the water and substrate layers (Wright and Hopky 1998):

$$T = \frac{2(Z_W / Z_S)}{1+(Z_W / Z_S)} \tag{19}$$

where Zw and Zs are the acoustic impedances in the water and substrate respectively. The acoustic impedance is calculated as a product of density and P-wave velocity and the cosine of the angle of propagation relative to the seabed. The highest amplitude entering the water column occurs for incident waves with small grazing angles, i.e. where the blast pressure wave propagates almost parallel to the seabed. According to Snell's law, the angle of propagation on the transmitted wave varies between 90° from the seabed (i.e., strait up and down in the water column) to 60° from the seabed for incident waves with small grazing angles. This conservative case (small grazing angles) was used for the pressure and impulse calculations.

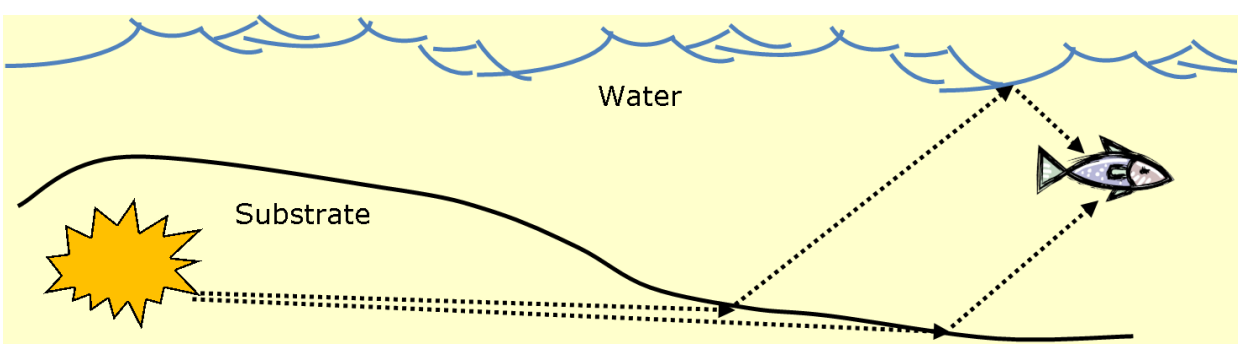

Figure 6. Diagram of pressure wave paths to a receiver in the water column (not to scale).

The transmitted wave, propagating at approximately 60º from the seabed will be reflected at the water surface. The sea-surface reflections will produce opposite-phase signals that truncate the positive phase of the transmitted direct-path pressure pulse, thereby reducing the impulse time integration window (Equation 13), without reducing the peak pressure. By calculating the peak pressure and impulse at the seabed the time delay between the direct and surface-reflected waves is maximized, thus representing a conservative measure for both peak pressure and impulse.

The approach to shockwave modeling adopted here does not take into account the variation of the bathymetry around the rock removal site.

2.3. Sound Propagation Models

Underwater sound propagation (i.e., transmission loss) at frequencies of 10 Hz to 20 kHz was predicted with JASCO's Marine Operations Noise Model (MONM). MONM computes received SEL for directional impulsive sources at a specified source depth.

2.3.1. Marine Operations Noise Model

At frequencies ≤ 2 kHz, MONM computes acoustic propagation via a wide-angle parabolic equation solution to the acoustic wave equation (Collins 1993) based on a version of the U.S. Naval Research Laboratory's Range-dependent Acoustic Model (RAM), which has been modified to account for an elastic seabed. The parabolic equation method has been extensively benchmarked and is widely employed in the underwater acoustics community (Collins et al. 1996). MONM-RAM accounts for the additional reflection loss at the seabed due to partial conversion of incident compressional waves to shear waves at the seabed and sub-bottom interfaces, and it includes wave attenuations in all layers. MONM incorporates the following site-specific environmental properties: a bathymetric grid of the modeled area, underwater sound speed as a function of depth, and a geoacoustic profile based on the overall stratified composition of the seafloor.

MONM-RAM's predictions have been validated against experimental data in several sound source verification programs conducted by JASCO (Hannay and Racca 2005, Aerts 2008, Funk et al. 2008, Ireland et al. 2009, O'Neill et al. 2010, Warner et al. 2010).

At frequencies ≥2 kHz, MONM employs the widely-used BELLHOP Gaussian beam ray-trace propagation model (Porter and Liu 1994) and accounts for increased sound attenuation due to volume absorption at these higher frequencies following Fisher and Simmons (1977). This type of attenuation is significant for frequencies higher than 5 kHz and cannot be neglected without noticeable effect on model results at long ranges from the source. MONM-BELLHOP accounts for the source directivity, specified as a function of both azimuthal angle and depression angle. MONM-BELLHOP incorporates site-specific environmental properties such as a bathymetric grid of the modeled area and underwater sound speed as a function of depth. In contrast to MONM-RAM, the geoacoustic input for MONM-BELLHOP consists of only one interface, namely the sea bottom. This is an acceptable limitation because the influence of the bottom sub-layers on the propagation of acoustic waves with frequencies above 2 kHz is negligible.

MONM computes acoustic fields in three dimensions by modeling transmission loss within two-dimensional (2-D) vertical planes aligned along radials covering a 360° swath from the source, an approach commonly referred to as N×2-D. These vertical radial planes are separated by an angular step size of $\Delta\theta$, yielding $N = 360°/\Delta\theta$ number of planes.

MONM treats frequency dependence by computing acoustic transmission loss at the center frequencies of 1/3-octave bands. Sufficiently many 1/3-octave bands, starting at 10 Hz, are modeled to include the majority of acoustic energy emitted by the source. At each center frequency, the transmission loss is modeled within each vertical plane (N×2-D) as a function of depth and range from the source. Third-octave band received (per-pulse) SELs are computed by subtracting the band transmission loss values from the directional source level (SL) in that frequency band. Composite broadband received SELs are then computed by summing the received 1/3-octave band levels.

The received SEL sound field within each vertical radial plane is sampled at various ranges from the source, generally with a fixed radial step size. At each sampling range along the surface, the sound field is sampled at various depths, with the step size between samples increasing with depth below the surface. The step sizes are chosen to provide increased coverage near the depth of the source and at depths of interest in terms of the sound speed profile. The received SEL at a surface sampling location is taken as the maximum value that occurs over all samples within the water column below, i.e., the maximum-over-depth received SEL. These maximum-over-depth SELs are presented as color contours around the source.

An inherent variability in measured sound levels is caused by temporal variability in the environment and the variability in the signature of repeated acoustic impulses (sample sound source verification results are presented in Figure 7). While MONM's predictions correspond to the averaged received levels, precautionary estimates of the radii to sound level thresholds are obtained by shifting the best fit line (solid line in Figure 7) upward so that the trend line encompasses 90% of all the data (dashed line in Figure 7).

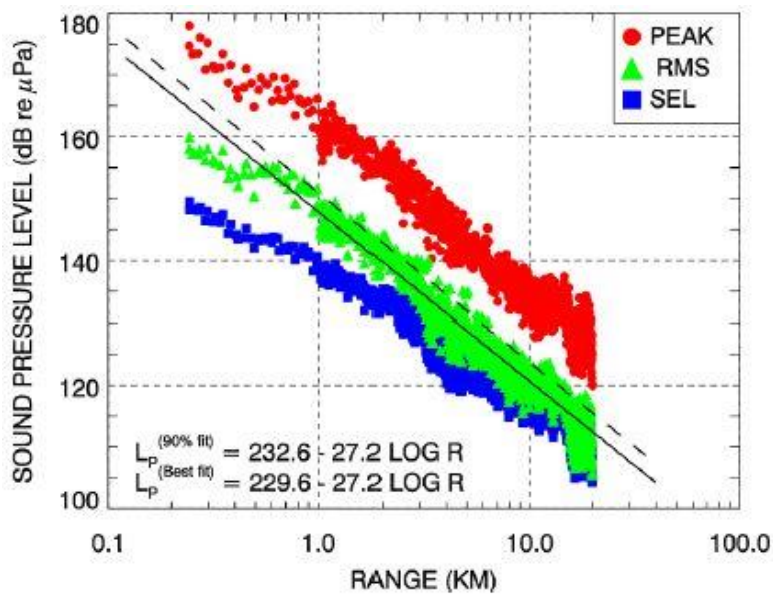

Figure 7. Peak and root-mean-square (rms) sound pressure level (SPL) and sound exposure level (SEL) versus range from a 20 in^3 airgun array. Solid line is the least squares best fit to rms SPL. Dashed line is the best-fit line increased by 3.0 dB to exceed 90% of all rms SPL values (90th percentile fit) (Ireland et al. 2009, Fig. 10).

2.3.2. Cumulative Sound Exposure Levels

While some impact criteria are based on per-pulse received energy at the subject's location, others account for the total acoustic energy to which marine life is subjected over a 24 h period. An accurate assessment of the cumulative acoustic field depends not only on the parameters of each pulse, but also on the number of pulses delivered in a given time period and the relative source position of the pulse. Quite a different issue, which is not considered here but bears mentioning as a qualifier to any estimates, is that individuals of most species would not remain stationary throughout the accumulation period, so their dose accumulation would depend also on their motion.

For vibratory pile driving and non-explosive rock removal operations that produce continuous not impulsive sound, cSEL is calculated by summing (on a logarithmic scale) the SEL that represents 1 s of operation over the total number of operational seconds expected in 24 hours.

3. Model Parameters

3.1. Environmental Parameters

3.1.1. Bathymetry

Water depths throughout the modeled area were obtained from soundings collected by the U.S. Army Corps of Engineers in support of the New Bedford Harbor Superfund Project. These soundings were adjusted to match proposed dredged depth in the pile driving area. In areas where no soundings were available, data were obtained from STRM30+ (v7.0), a global topography and bathymetry grid with a resolution of 30 arc-seconds or about 2,300 × 6,000 ft (700 × 1,800 m) at the studied latitude (Rodriguez et al. 2005).

Bathymetry for a 10 × 12 miles (16 × 19 km) area, including waters from the Acushet River to Buzzards Bay, was re-gridded by minimum curvature gridding onto a Universal Transverse Mercator (UTM) Zone 19 projection with a horizontal resolution of 6.6 × 6.6 ft (2 × 2 m). Note that all maps presented in this report were projected onto the horizontal datum NAD 1983 U.S. State Plane Massachusetts Mainland Zone 19 (feet).

3.1.2. Geoacoustics

MONM assumes a single geoacoustic profile of the seafloor for the entire model area. The acoustic properties required by MONM are:

- sediment density,
- compressional-wave (or P-wave) sound speed,
- P-wave attenuation in decibels per wavelength,
- shear-wave (or S-wave) speed, and
- S-wave attenuation, in decibels per wavelength.

The geological stratification in New Bedford Harbor was based on boring logs provided by Apex. In general, dark grey sand with some grey to black organic silt was found down to 10–35 ft below the mudline. Based on the available data, this layer was averaged to 21 ft below the mudline for modeling purposes. Throughout the harbor, fractured grey granite bedrock (gneiss) is found directly below the silty sand layer. Seismic refraction data collected by Northeast Geophysical Services in March 2011 provided estimates of P-wave sound speed in this gneiss layer.

The other necessary acoustic properties were estimated from the geological stratification and sound speed data provided by Apex and values from analysis of similar material by Hamilton (1980), Ellis and Hughes (1989), and Barton (2007). Table 3 presented the geoacoustic profile used by the sound propagation model MONM. Table 4 presents the geoacoustic parameters used by the semi-empirical model ConWep.

Table 3. Estimated geoacoustic profile for Sites 1 and 2. Within each sediment layer, parameters vary linearly within the stated range.

Depth below seafloor (ft)	Material	Density (lb/ft^3)	P-wave speed (ft/s)	P-wave attenuation (dB/λ)	S-wave speed (ft/s)	S-wave attenuation (dB/λ)
0-21	Sand and some black organic silt	110.5-121.7	5,331-7,150	0.96-1.10	1,180	4.8
21-27	Grey granite Gneiss	162.3	10,250-16,807	0.275		
≥ 27	Grey granite Gneiss	162.3	16,807	0.275		

Table 4. Estimated geoacoustic parameter for grey granite bedrock (gneiss) found in Dredge areas 2 and 3 (Figure 1).

Material	Density (lb/ft^3)	P-wave speed (ft/s)	Attenuation coefficient
Grey granite gneiss	162.3	10,250	1.9

3.1.3. Sound Speed Profile

The sound speed profiles for the modeled sites were derived from sound speed profile data provided by Apex (Figure 8). These profiles were verified against temperature and salinity profiles from the US Naval Oceanographic Office's *Generalized Digital Environmental Model V 3.0* (GDEM; Teague et al. 1990, Carnes 2009). GDEM provides ocean climatology of temperature and salinity for the world's oceans on a latitude-longitude grid with 0.25° resolution, with a temporal resolution of one month, based on global historical observations from the US Navy's Master Oceanographic Observation Data Set (MOODS). The climatology profiles include 78 fixed depth points, up to a maximum depth of 22,310 ft (6,800 m) (where the ocean is that deep), including 55 standard depths between 0 and 6,562 ft (2,000 m). The GDEM temperature-salinity profiles were converted to sound speed profiles according to the equations of Coppens (1981):

$$\begin{aligned} c(z,T,S,\phi) &= 1449.05 + 45.7t - 5.21t^2 - 0.23t^3 \\ &\quad + \left(1.333 - 0.126t + 0.009t^2\right)(S-35) + \Delta \\ \Delta &= 16.3Z + 0.18Z^2 \\ Z &= \frac{z}{1000}\left(1 - 0.0026\cos(2\phi)\right) \\ t &= \frac{T}{10} \end{aligned} \tag{20}$$

where z is water depth (m), T is temperature (°C), S is salinity (psu), and ϕ is latitude (radians).

The same monthly variations were observed in both Apex and GDEM data. Since Apex data were sampled within the New Bedford Harbor, and GDEM data were only available within Buzzard Bay, Apex's sound speed profiles are used to provide a more accurate estimate of the sound speed at the South Terminal Project sites.

To provide precautionary estimates of distances to level thresholds, sound propagation was modeled for the month of September (yellow, Figure 8). The sound speed profile in fall becomes

slightly upward refractive, which promotes sound propagation by reducing interactions with the seabed.

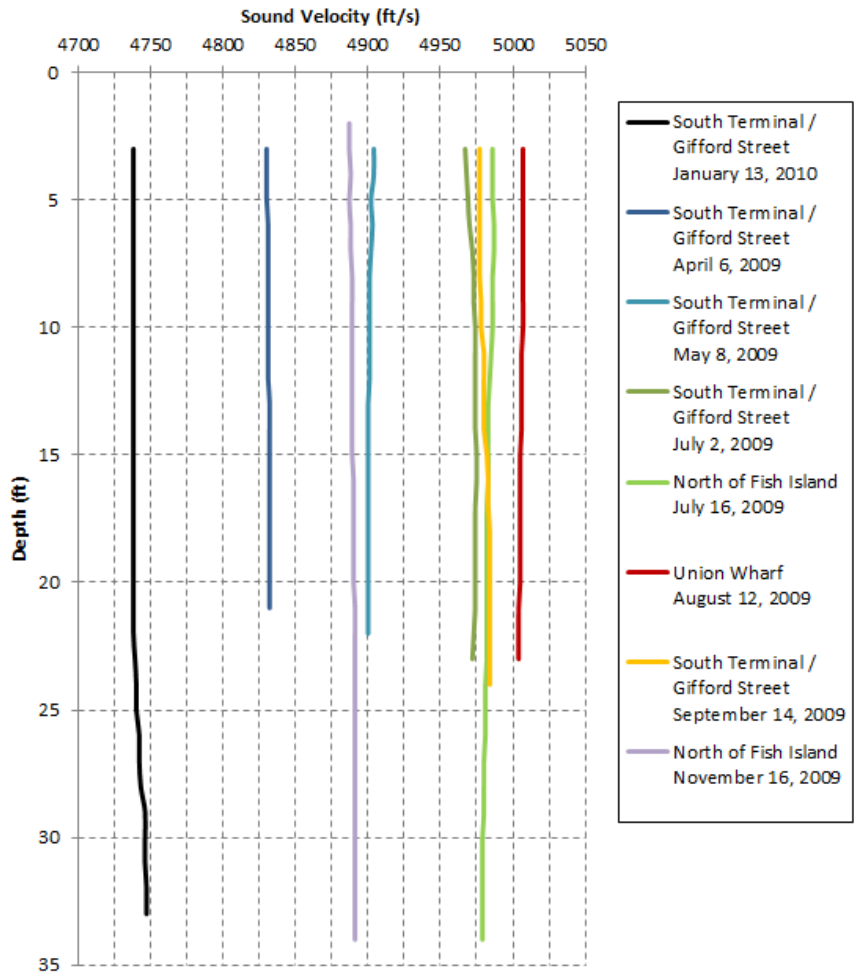

Figure 8. Sound speed profiles sampled at various locations and times of year within New Bedford Harbor, MA.

3.2. Geometry and Modeled Volume

The sound fields were modeled over New Bedford Harbor on an area about 13,123 × 23,950 ft (4.0 × 7.3 km), with a horizontal separation of 6.6 ft (2 m) between receiver points along the modeled radials. Sound fields were modeled with a horizontal angular resolution of $\Delta\theta = 2.5°$, for a total of $N = 144$ radial planes. The receiver depths span the entire water column over the modeled areas, from 1 to 164 ft (0.3 to 50 m), with step sizes that increased from 0.3 to 16.4 ft (0.1 to 5 m), with increasing depth.

4. Results

4.1. Source Levels

4.1.1. Pile Driving

Blackwell et al. (2007) provided received sound level spectra from vibratory pile driving. This spectrum revealed distinct peaks in the 1/3-octave bands centered at 16, 31.5, and 50 Hz, which are consistent with the vibration frequency of about 30 Hz. The spectrum was scaled to a broadband level equal to the maximum source level for vibratory pile driving a 24-inch (0.6 m) pile reported by Illingworth & Rodkin (2007): 185 dB re 1 µPa^2·s.

Since the 24–36 inch diameter steel piles are to be set into pre-drilled holes, 1/3-octave bands source levels were also estimated for the drilling operation. JASCO recorded a Beetle (hammer) drill with a drill bit diameter of 24 inches passing through metamorphic rock (Mouy and Zykov 2009). The drill rig was installed on a temporary metal frame resting on the river bottom. This hammer-drilling operation and environment are expected to be representative of the activities proposed for the New Bedford terminal.

Figure 9 presents resultant source level spectra in 1/3-octave bands. Since the broadband levels are estimated higher for pile driving operations than for drilling operations, the spectrum for vibratory hammers was used in this study.

As the pile flexes under the action of the pile driver, its entire length excites pressure waves in the water, meaning that the pile is a distributed sound source. Because of losses from bottom and surface interactions, attenuation will be less for a source at mid-depth than for one near the seafloor or surface. The pile was approximated by a point source located at half the water depth. This positioning of the equivalent point source is estimated to result in precautionary distances to sound level thresholds.

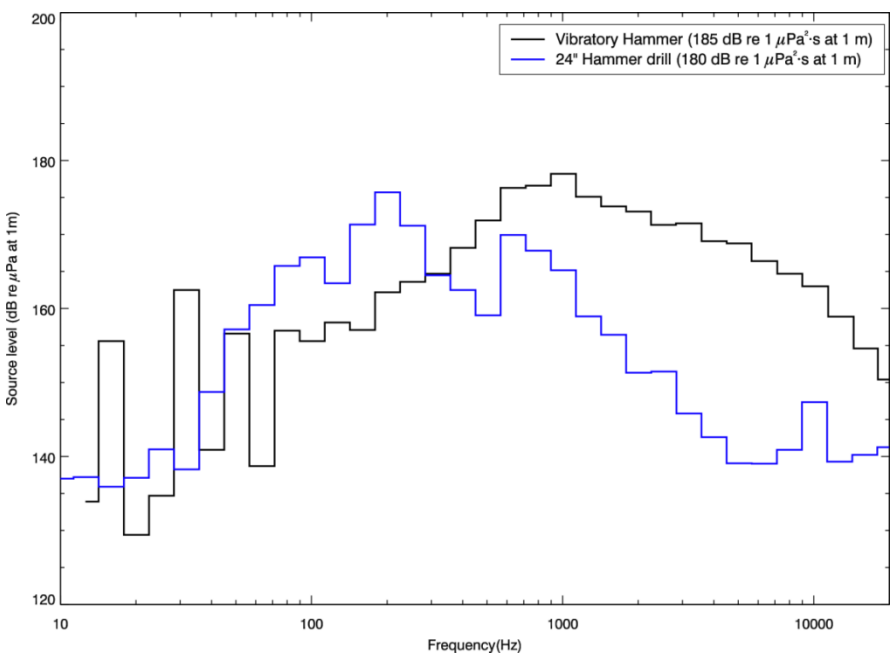

Figure 9. Estimated 1/3-octave band source level spectra for pile driving operations.

4.1.2. Rock Removal–Non-Explosive

Since underwater spectrum representing hydraulic impact hammering (Hoe Ram) and drilling and fracturing of metamorphic rock were not found in the literature, a Beetle (hammer) drill with a drill bit diameter of 24 inches passing through metamorphic rock (Mouy and Zykov 2009), was used as proxy for the two types of activities.

A cutter-head may also be used to help loosen the sediments. The head can usually be steered using cables and winches or thrusters. Generally, cutter-head dredges do not have a propulsion system, but use *legs*, known as spuds, to swing between anchors, or may use service tugs. The major source of noise is generated by the impact and abrasion of the sediment passing through the cutter-head, suction pipe, and pump (Robinson et al. 2011).

Backhoe dredgers are relatively quiet compared to other dredges (CEDA 2011). The noise sources from backhoe dredging are the barge-installed power plant and scraping sounds as the bucket digs into hard sediment. Backhoe and bucket dredgers have a similar setup: a crane installed on a barge. The only difference being that the bucket is controlled through a steel wire cable instead of a rigid arm. Since noise measurements of a backhoe dredger were unavailable, clamshell bucket dredge measurements were used as proxy.

One dredging duty cycle for a clamshell bucket dredge involves the following events:

- Bucket striking the bottom,
- Bucket digging into the bottom/bucket closing,
- Winching up, and
- Dumping the material from the bucket.

Dickerson et al. (2011) identified that the noisiest event is the bucket striking the bottom. This acoustic event is very short compared to the length of a duty cycle (~1 min), and happens once per duty cycle. The source levels for other events are at least 6 dB lower. Table 5 presents the specification for the cutter-head and clamshell bucket dredges considered in this study. Figure 10 presents the 1/3-octave band source level spectra for cutter-head dredges, clamshell bucket dredges, and a 24-inch hammer drill.

Table 5. Dredges Specifications.

Dredge Name	Type	Length × breath × draft (ft)	Capacity	Pump power (kW)	Dredging depth (ft)	Estimated rms SPL broadband level (dB re 1 µPa @ 1 m)	Reference
JFJ de Nul	Cutter-head suction dredge using thruster to move cutter-head	408 × 91 × 21	unknown	Cutter drive: 6000 Submerged dredge pump on cutter ladder: 3800 Inboard dredge pumps: 2 x 6000 Propulsion: 2 x 3800 Total installed power: 27 190	19 (min) 115 (max)	179.6	Hannay et al. 2004 and http://www.sakhalinenergy.com/en/documents/doc_33_cea_tbl4-7.pdf
Aquarius	Self-propelled Cutter-head suction dredge using thrusters to move cutter-head	351 × 62 × 16	unknown	unknown	82 (max)	185.5	Malme et al. 1989
Columbia	Cutter-head suction dredge using winch to move cutter-head	160 × 44 × 7	unknown	Cutter power: 375 Total power: 3954 Pipe Diameter: 2 ft	59 (max)	181.8	McHugh et al. 2007
Beaver MacKenzie	Cutter-head suction dredge using winch to move cutter-head	284 × 51 × 13	Gross tonnage: 2148.5 t	Ladder: 1119 (1500 hp) Discharge: 1268 (1700 hp) jet pump: 1119 (1500 hp) Pipe Diameter: 2.8 ft	148 (max)	172.1	Malme et al. 1989
Viking	Clamshell bucket dredge	260 × 66 × 6	Maximum lift : 136 t	unknown	unknown	169.5	Dickerson et al. 2001
Argilopotes	Clamshell bucket dredge	unknown	unknown	unknown	unknown	167.6	Miles et al. 1987

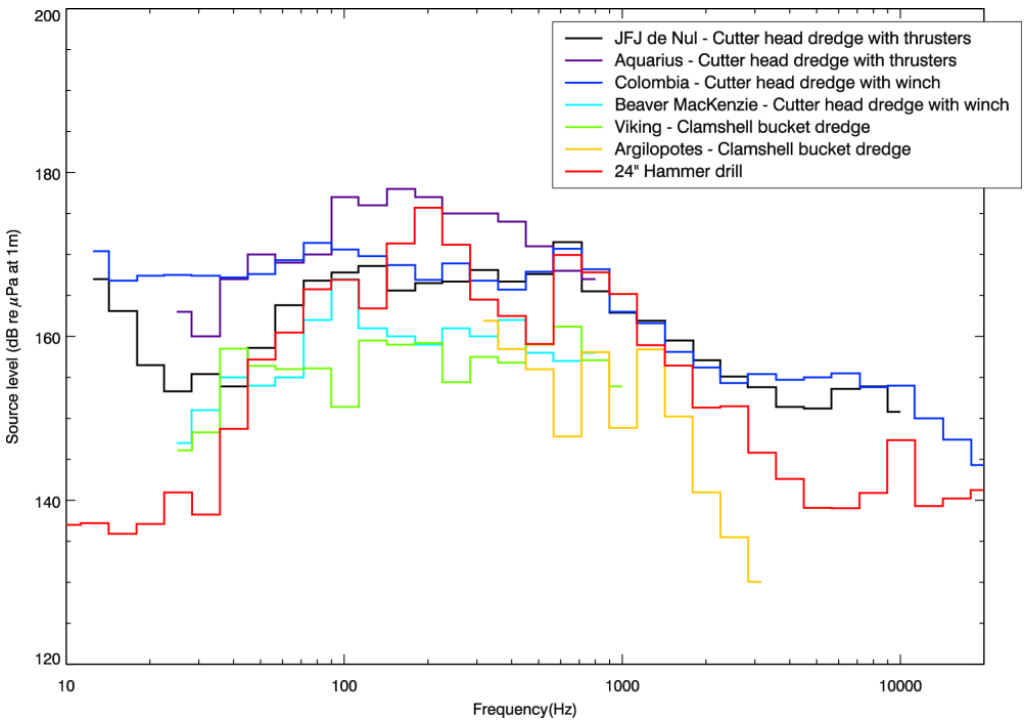

Figure 10. Estimated 1/3-octave band source level spectra for cutter-head dredges, clamshell bucket dredges, and a 24-inch hammer drill.

Sound levels from the cutter-head dredge Aquarius were used in this study, since they represents the highest broadband source levels (185.5 dB re 1 µPa @ 1 m). As the available spectrum for Aquarius does not include frequencies above 800 Hz, source levels at higher frequencies were estimated using the highest values in each 1/3-octave band between the cutter-head dredges JFJ de Nul and Colombia.

Because losses from bottom and surface interactions will be less for a source at mid-depth than for one near the seafloor or surface, the sound of non-explosive rock removal activities was approximated by a point source located at half the water depth. This positioning of the equivalent point source is estimated to produce results in precautionary distances to level thresholds.

4.1.3. Rock Removal–Explosive

The original peak pressure and impulse of the shock wave from explosive rock removal operation were predicted with UnderWater Calculator (Dzwilewski and Fenton 2003). Equations 17 and 18 calculate the peak pressure and impulse values of the shockwave from a blast. The calculations were done for the distances as far as 4500 ft from the detonation point. Scenarios were considered with charge sizes of 30, 50, 100, 130 and 150 lbs. Scenarios with a charge inside a pipe were considered to provide estimates of a buried charge. Coupling efficiency of a charge placed inside bedrock was estimated to vary with the charge size from 38.0% for a 30-lbs charge to 52.4% for a 150-lbs charge.

The most recent blast specification (Section 2.2.3) mention that Blastex Plus TX will be used. Since this material is not present in the ConWep database, ANFO was used as charge material. Based on the Blastex Plus TX material safety data sheet, it is made of similar material as ANFO

but specially packed for use in wet environments. Five charge weights (30, 50, 100, 130, and 150 lb) were modeled. Based on the information provided in the August 2013 Operational Blasting Plan, the top of the charge was estimated to be between 3 and 18.8 ft below the seafloor (considering overburden and capping material). On precautionary grounds the detonation depth was modeled at the shallowest burial depth of 3 ft since a shallower detonation is expected to produce higher peak pressure and impulse levels.

Figure 11 shows an example of modeled pressure waves at 38–160 ft from the detonation of a 30-lbs charge. These modeled pressure waves were used to calculate peak pressure and impulse levels away from the detonation. Based on these calculations, the adjusted coupling efficiency of a charge placed inside bedrock was estimated to vary between 2.25% and 5.5%, depending on the charge size.

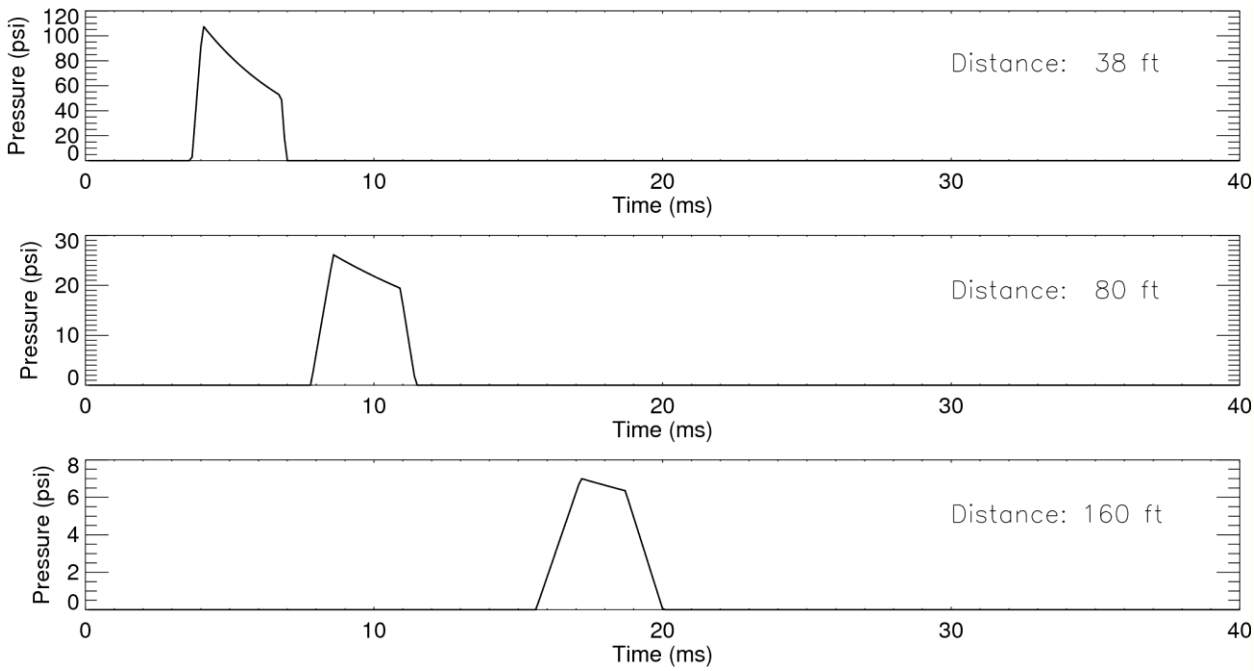

Figure 11. Modeled pressure waveform at the seabed, at a distance of 38, 80, and 160 ft from the detonation of a 30-lb charge.

4.2. Sound Fields

It is important to note that several assumptions were made to estimate precautionary distances to sound level thresholds. In addition to the assumptions detailed in Sections 2, 3, and 4.1, the water column was assumed free of obstructions such as construction barges or other vessels that could act as partial noise barriers, depending on their draft. The underwater sound fields predicted by the propagation model were also sampled such that the received sound level at each point in the horizontal plane was taken to be the maximum value over all modeled depths for that point (see Section 2.3.1).

The predicted distances to specific sound level thresholds were computed from the maximum-over-depth sound fields. The model results are presented as contour maps of maximum-over-

depth rms SPL in 10 dB steps, and contours to maximum-over-depth peak SPL, cSEL, and rms SPL thresholds, or peak pressure and impulse level thresholds. Distances to specified threshold are recorded in the legend of the contour maps for pile driving and non-explosive rock removal operations, and tabulated for rock removal operations using explosives.

For pile driving and non-explosive rock removal operations, two distances from the source are reported for sound levels representing the selected impact criteria: (1) R_{max}, the maximum range at which the given sound level was encountered in the modeled sound field; and (2) $R_{95\%}$, the maximum range at which the given sound level was encountered after exclusion of the 5% farthest such points. This definition is meaningful in terms of impact on marine life, because, regardless of the geometric shape of the noise footprint for a given sound level threshold, $R_{95\%}$ is the predicted range encompassing at least 95% of animals of a uniformly distributed population would be exposed to sound at or above that level.

4.2.1. Pile Driving

Apex estimates that each pile will to be driven into place in about 10 min using a vibratory hammer. Cumulative SEL was calculated assuming 10 min of vibratory hammer pile driving operation for each of the 16 piles to be driven in a 24-hour period. Thus, cSELs presented here assume 9600 s of operation in 24 hours. Peak SPL for vibratory pile driving is not expected to reach 206 dB re 1 µPa.

Figure 12 presents a contour map of the modeled rms SPL for pile driving operation with vibratory hammer. Figure 13 presents a contour map of the modeled sound level thresholds for that type operation.

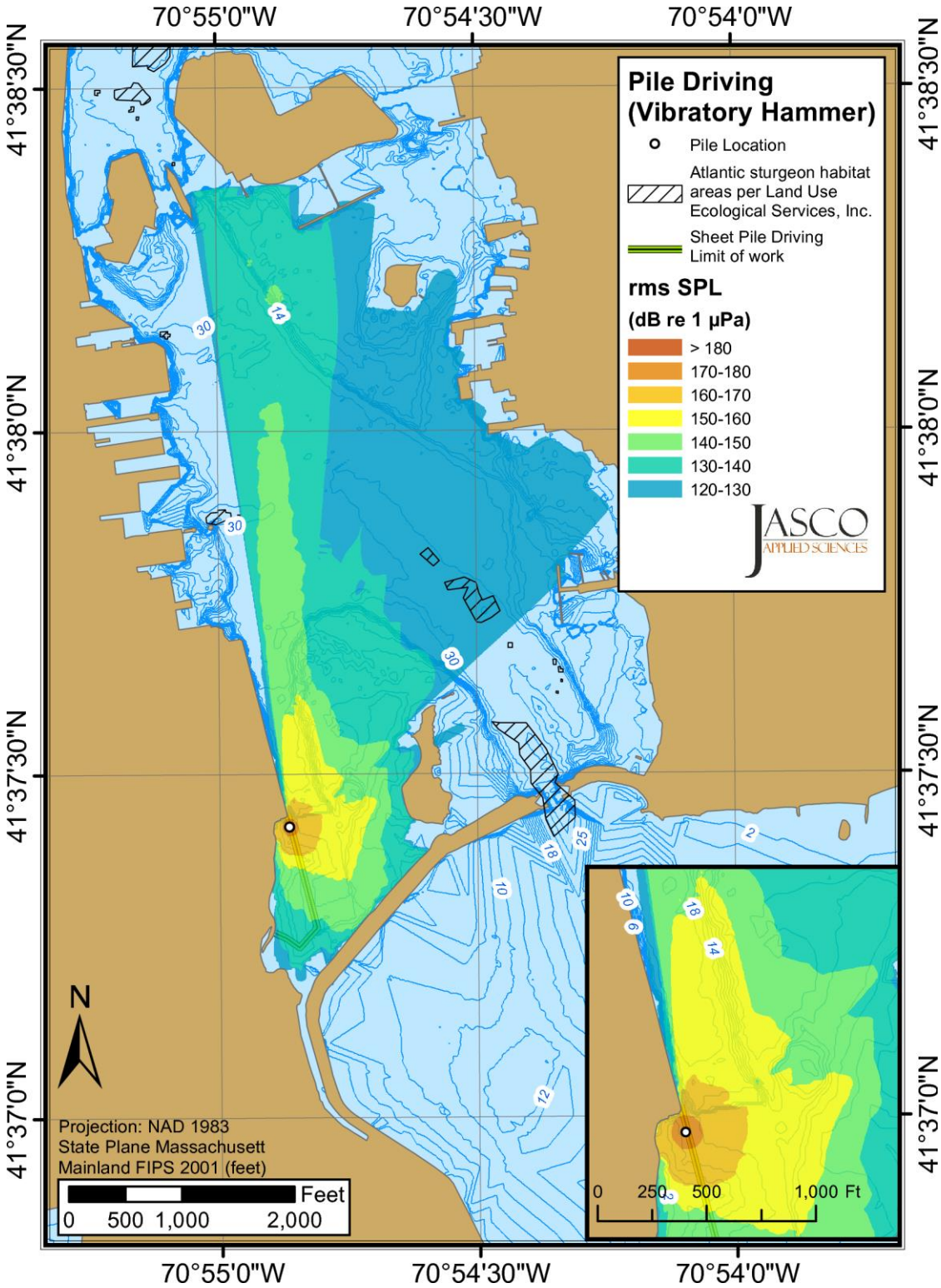

Figure 12. Pile driving with a vibratory hammer at Site 2: Received maximum-over-depth root-mean-square (rms) sound pressure levels (SPLs). Blue contours indicate water depth in feet.

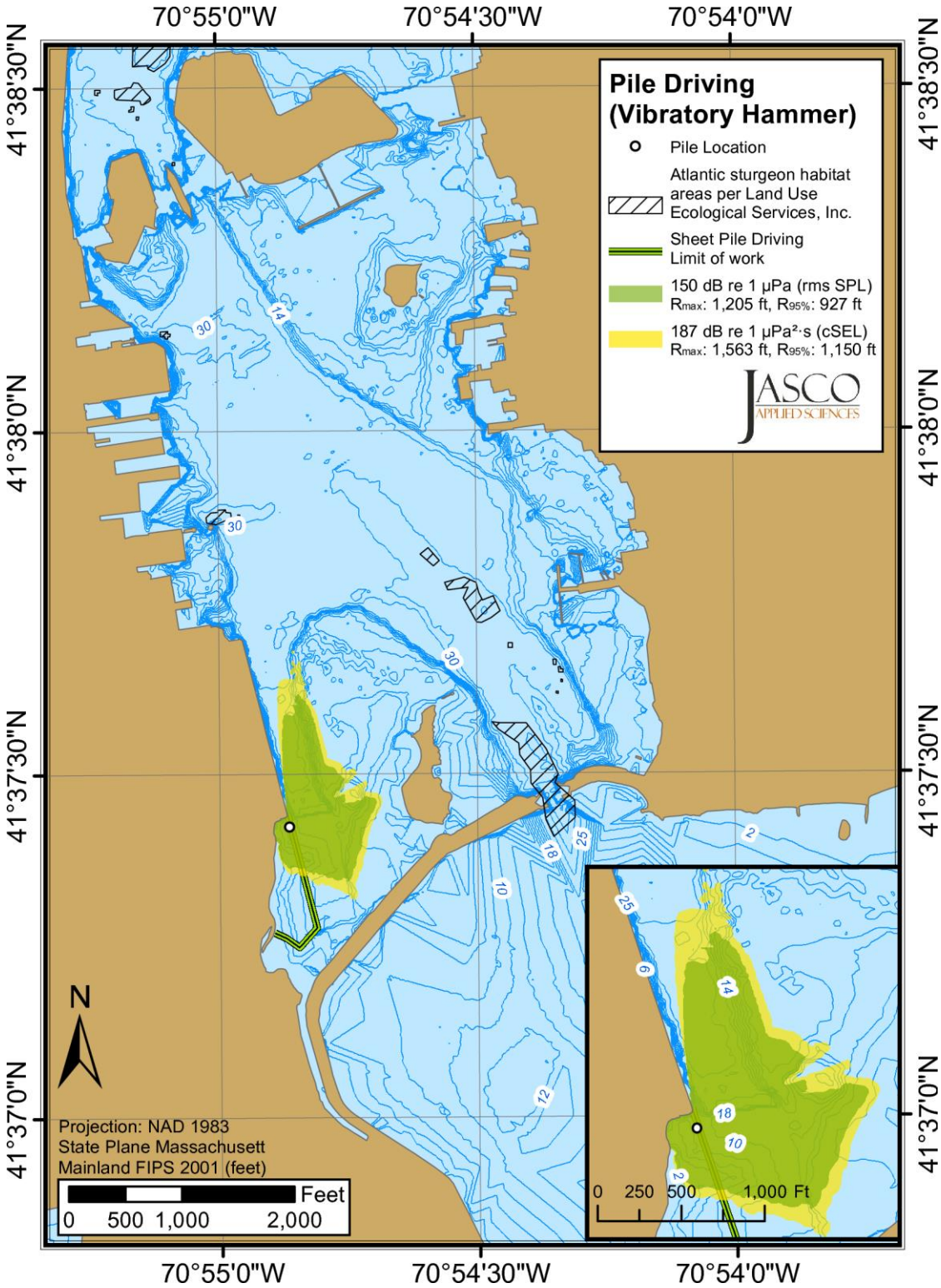

Figure 13. Pile driving with a vibratory hammer at Site 2: Received maximum-over-depth sound level thresholds. Blue contours indicate water depth in feet.

4.2.2. Rock Removal–Non-Explosive

Apex estimates 4 h of non-explosive rock removal operation. Thus, cSELs presented here assume 14 400 s of cutter-head dredge operation in 24 hours. Peak SPL for vibratory pile driving is not expected to reach 206 dB re 1 µPa.

Figures 14 and 16 present contour maps of the modeled rms SPL for non-explosive rock removal (using a cutter-head dredge), while Figures 15 and 17 present contour maps of the modeled sound level thresholds for same type of operation.

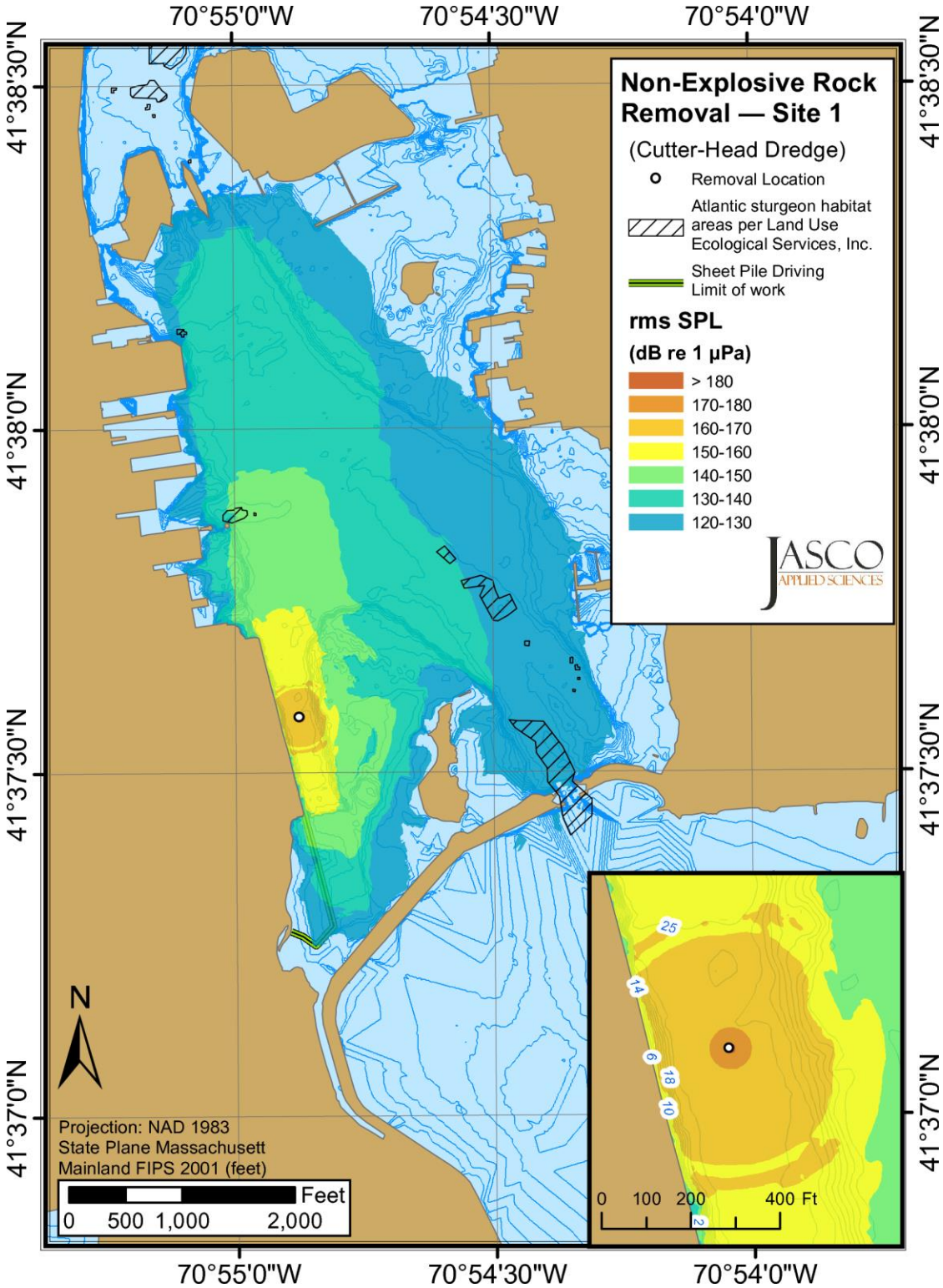

Figure 14. Non-explosive rock removal at Site 1: Received maximum-over-depth root-mean-square (rms) sound pressure levels (SPLs). Blue contours indicate water depth in feet.

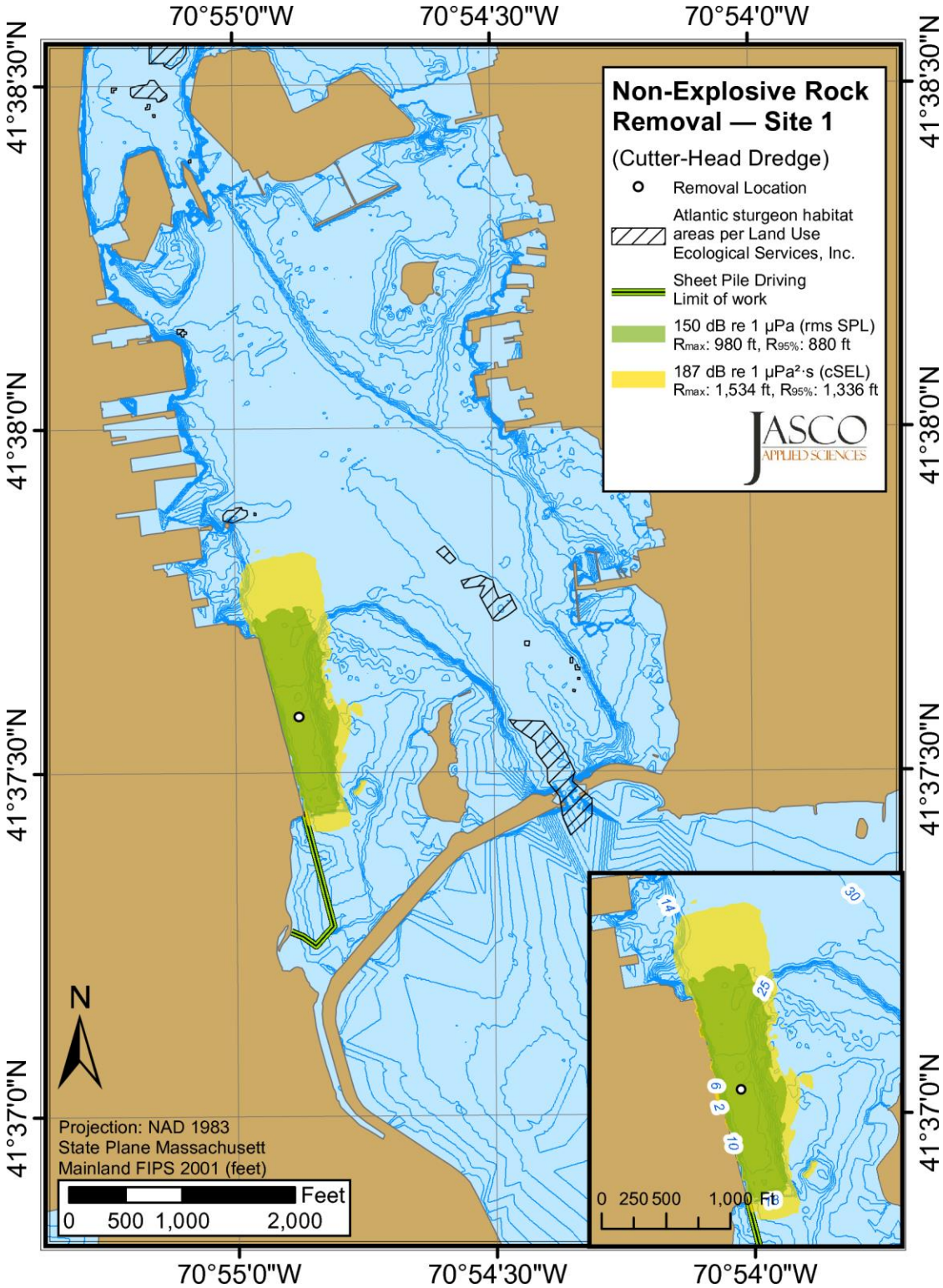

Figure 15. Non-explosive rock removal at Site 1: Received maximum-over-depth sound level thresholds. Blue contours indicate water depth in feet.

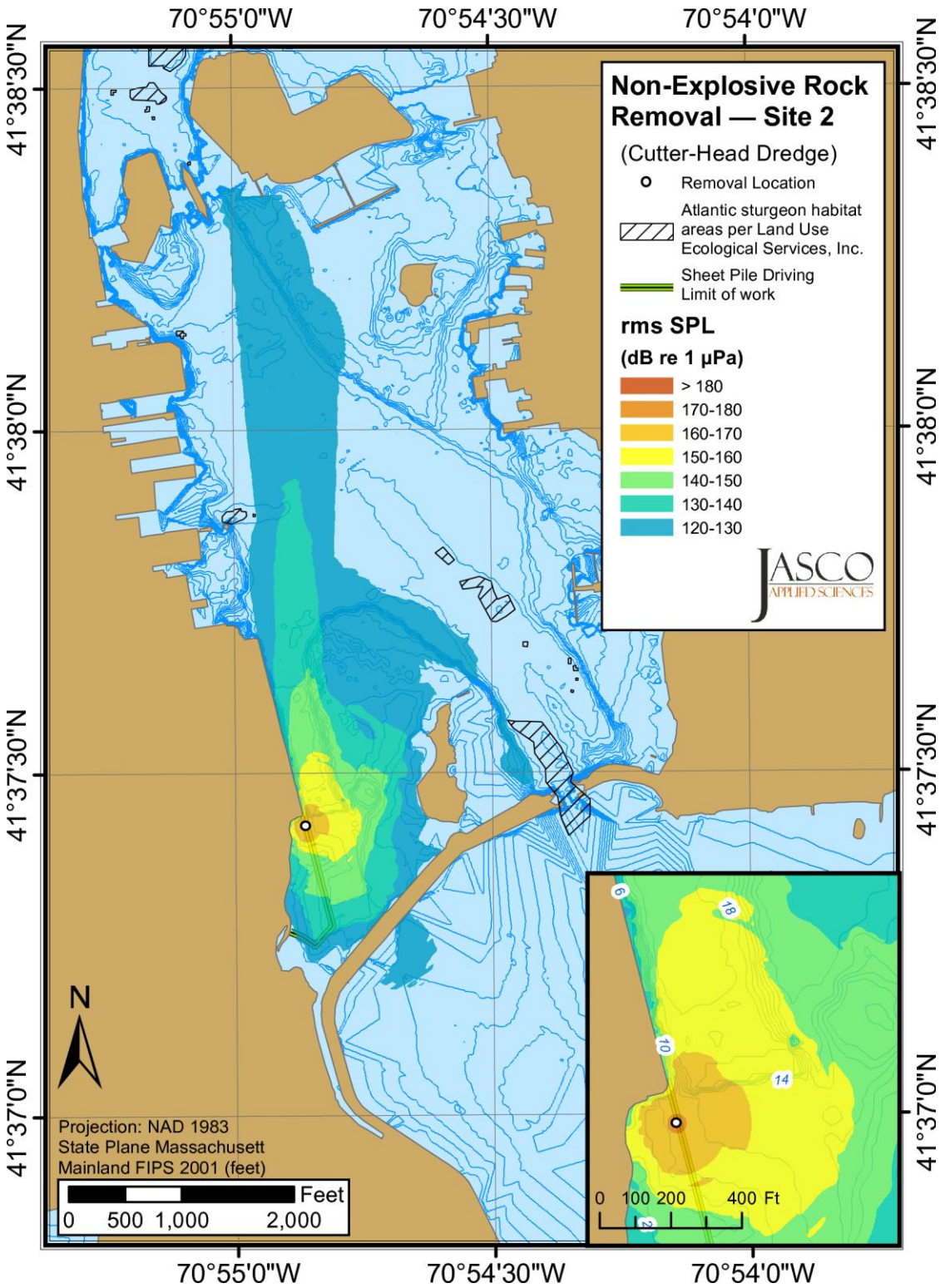

Figure 16. Non-explosive rock removal at Site 2: Received maximum-over-depth root-mean-square (rms) sound pressure levels (SPLs). Blue contours indicate water depth in feet.

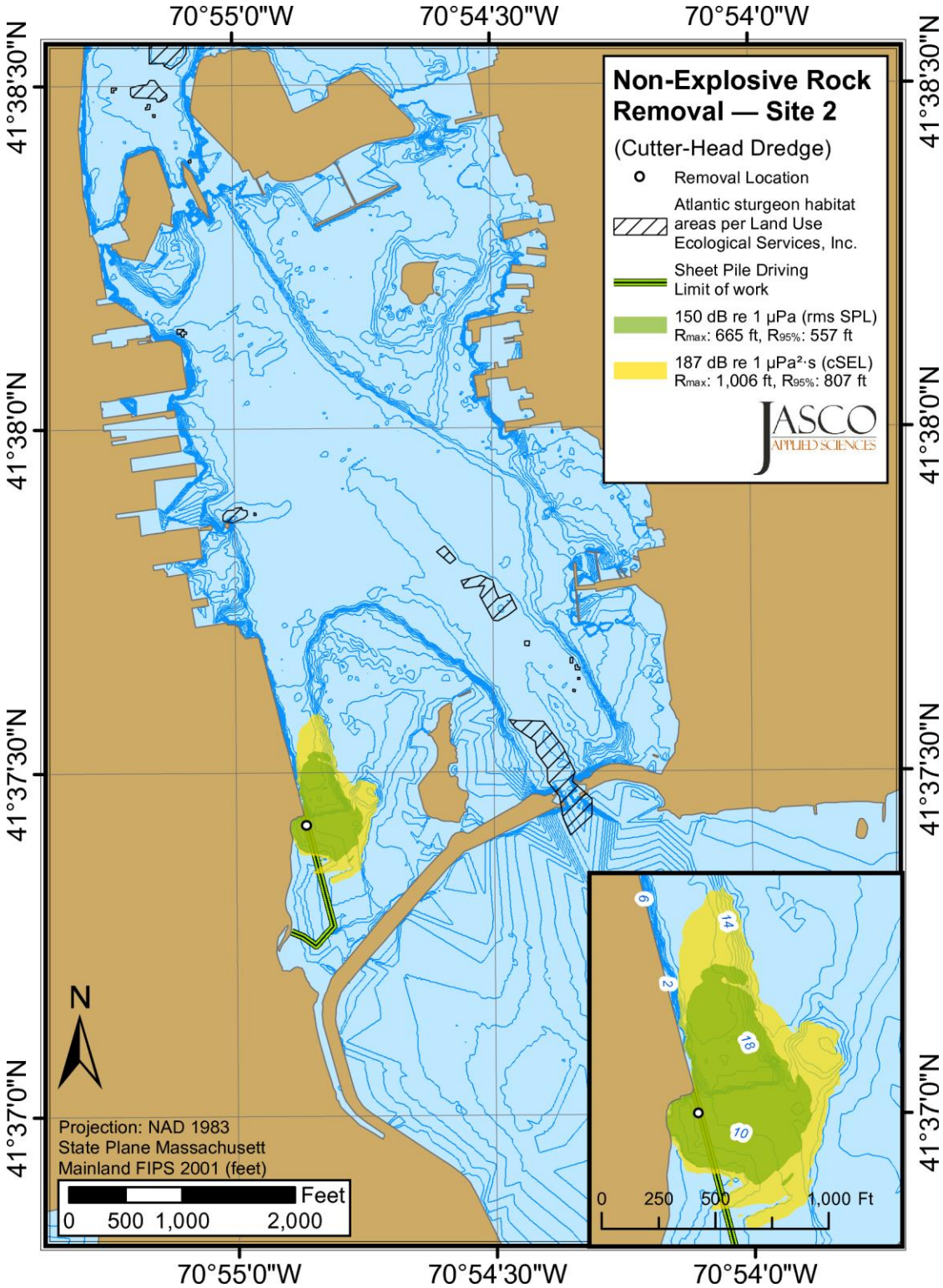

Figure 17. Non-explosive rock removal at Site 2: Received maximum-over-depth sound level thresholds. Blue contours indicate water depth in feet.

4.2.3. Rock Removal–Explosive

From a physical standpoint, the modeled distances to impulse levels for injury criteria (18.4 psi·s) can be validly considered as distances for charge weight per delay for delays of 25 ms or greater. This statement is based on the fact that the integration period for the impulse metric is defined as the time elapsed from the onset of the primary pressure wave to its return to ambient, i.e. the duration of the first positive pressure wave; this will be applicable individually to the events in a delayed sequence of detonations as long as the onset of an event does not overlap the positive phase of the previous one. While the positive pressure phase of an event may last just a few milliseconds, in practice some standard delay guidelines are generally applied to ensure a clear separation under realistic conditions. In the absence of formal directives from NMFS regarding minimum acceptable delays, and in the absence of details about the charge layout geometry for the construction activities for the New Bedford terminal, we recommend a minimum time delay of 25 ms between detonations based on Canadian guidelines for the use of explosives in or near fisheries waters (Wright and Hopky 1998) and experimental results presented by the National Marine Fisheries Services (NMFS; Bullard, J. K. 2012).

JASCO's analysis was limited to the physical estimate of acoustic parameters, and does not attempt to provide an interpretation of the biological impact on fish.

The distances to peak pressure and impulse thresholds estimated using the UnderWater Calculator spreadsheet (original and adjusted distances) and ConWep are presented in Tables 6 and 7. The adjusted distances to injury thresholds are also presented as contour maps in Figures 18 and 19.

The adjusted effective weight coefficients used in the UnderWater Calculator spreadsheet vary between 2.25% and 5.5%. These values are in accordance with the expected reduction in effects from buried blasts (USACE 1999). For all charges, the distance to impulse criterion exceeds the distance to peak pressure criterion. We note that the adjusted distances to the peak pressure threshold are conservative, as they exceed significantly the ConWep model estimates.

Although the formal modeling has been performed for Site 2, we estimate that the distances to injury thresholds for blasting operations presented here would be applicable to detonations located at Site 1. The geoacoustic properties within the dredge areas are very similar and would be modeled using the same parameters. Thus, in comparing the two environments, the major factor influencing the distances to injury criteria is the water depth, which is somewhat greater at Site 1. With increasing water depth, the time delay between the surface-reflected and direct pressure waves increases, causing the range to impulse threshold to be larger. The precautionary buffer applied to the presented results by using adjusted effective weight coefficients, however, should accommodate the variation in water depth between the two sites making the estimates representative for Site 1.

Table 6. Distances to peak pressure injury criterion of 75.6 psi.

Charge Weight (lbs)	Original (ft)	ConWep (ft)	Adjusted (ft)	Adjusted Effective weight coefficient
30	346	46	182	5.5%
50	418	53	201	4.5%
100	552	65	222	3%
130	617	70	228	2.5%
150	659	73	231	2.25%

Table 7. Distances to impulse injury criterion of 18.4 psi-msec.

Charge Weight (lbs)	Original (ft)	ConWep (ft)	Adjusted (ft)	Adjusted Effective weight coefficient
30	681	166	187	5.5%
50	1017	196	219	4.5%
100	1820	240	268	3%
130	2304	258	283	2.5%
150	2631	268	291	2.25%

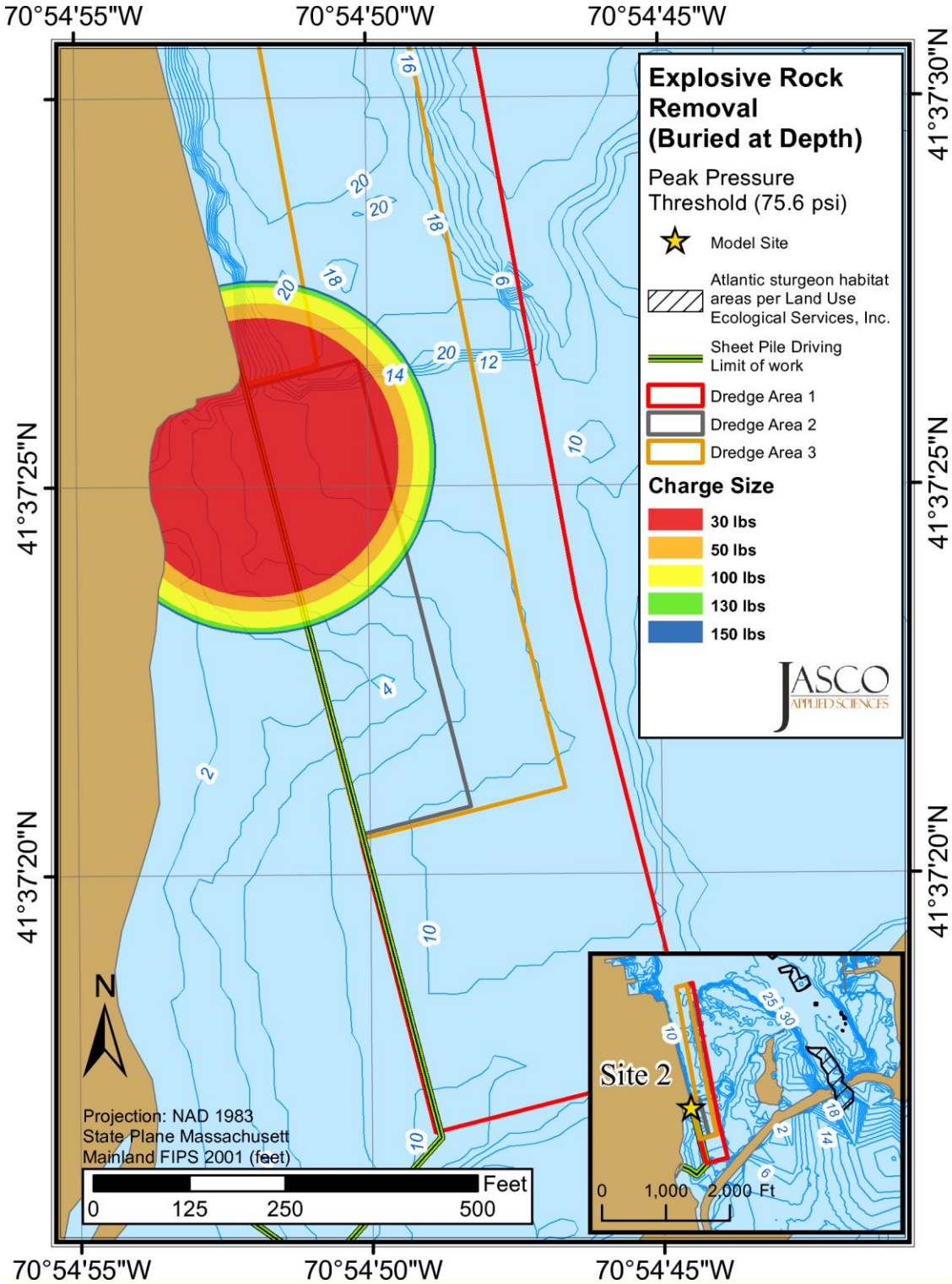

Figure 18. Explosive charge at Site 2: Peak pressure threshold of 75.6 psi for explosive charges between 30 and 150 lbs. Blue contours indicate water depth in feet.

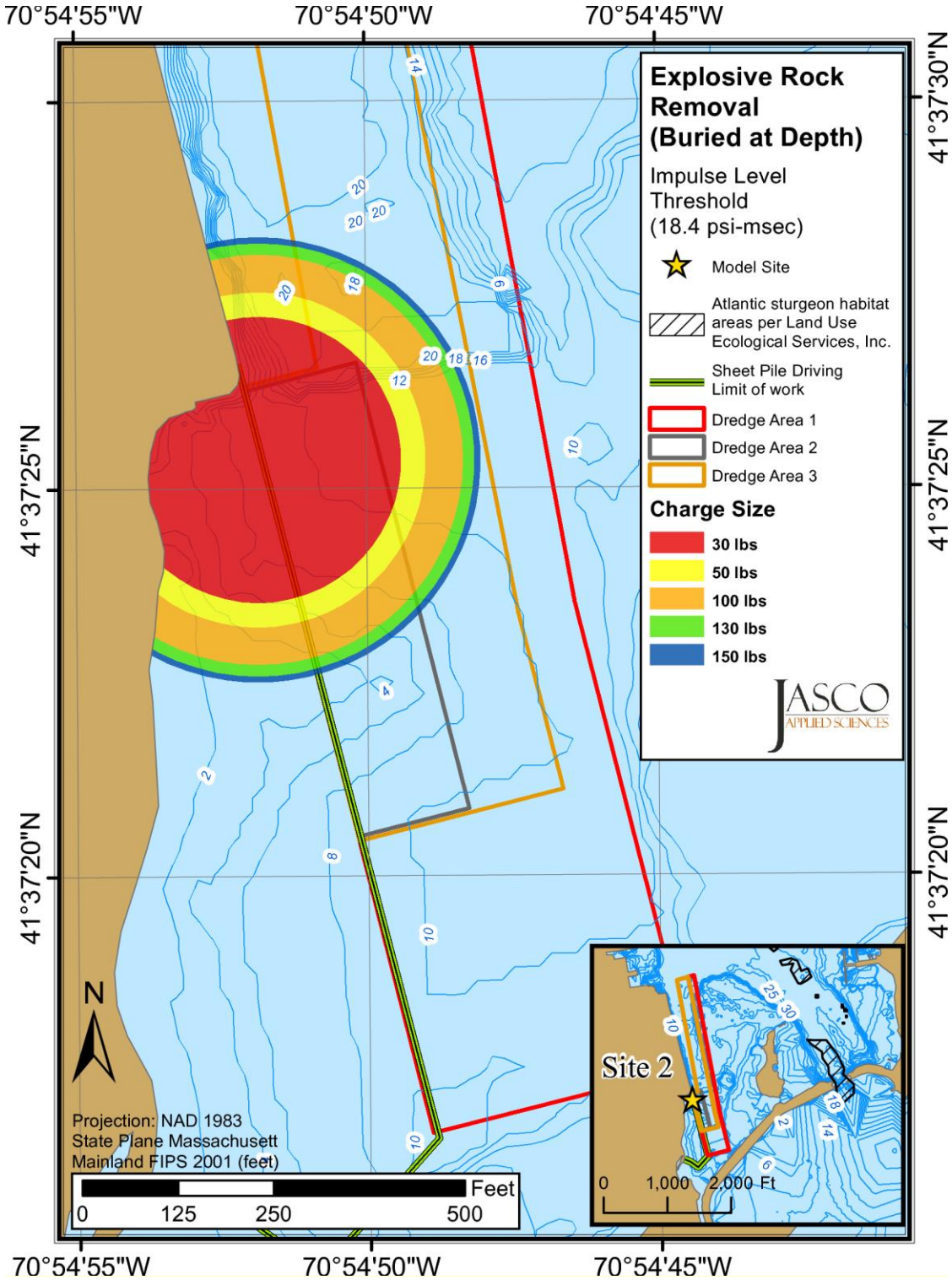

Figure 19. Explosive charge at Site 2: Impulse level threshold of 18.4 psi·msec for explosive charges between 30 and 150 lbs. Blue contours indicate water depth in feet.

Literature Cited

Aerts, L., M. Blees, S. Blackwell, C. Greene, K. Kim, D. Hannay, and M. Austin. 2008. *Marine mammal monitoring and mitigation during BP Liberty OBC seismic survey in Foggy Island Bay, Beaufort Sea, July-August 2008: 90-day report.* LGL Rep. P1011-1. Prepared by LGL Alaska Research Associates Inc., LGL Ltd., Greeneridge Sciences Inc. and JASCO Applied Sciences Ltd. for BP Exploration Alaska.

Austin, M., J. Delarue, H.A. Johnston, M. Laurinolli, D. Leary, A. MacGillivray, C. O'Neill, H. Sneddon, and G. Warner. 2009. *NaiKun Offshore Wind Energy Project Environmental Assessment*, Volume 4–Noise and Vibration. Technical report for NaiKun Wind Development Inc. by JASCO Applied Sciences.

Barton, N. 2007. *Rock Quality, Seismic Velocity, Attenuation, and Anisotropy*. Taylor & Francis, CIP Bath Press. 729 p.

Blackwell, S.B., R.G. Norman, C.R. Greene Jr., and W.J. Richardson. 2007. Acoustic measurements. (Chapter 4) *In*: *Marine Mammal Monitoring and Mitigation during Open Water Seismic Exploration by Shell Offshore Inc. in the Chukchi and Beaufort Seas, July–September 2006: 90-Day Report*. LGL Report P891-1. Report by LGL Alaska Research Associates Inc. and Greeneridge Sciences Inc. for Shell Offshore Inc., National Marine Fisheries Service (US), and US Fish and Wildlife Service. pp 4-1 to 4-52.

Betke, K. 2008. Minderung von Unterwassergeräuschen beim Bau von OffshoreWEA, BSH-Workshop FINO3, Hamburg, 8 Oct. 2008.

Bullard, J.K. 2012. RE: Route 52 Causeway Replacement & Somers Point Circle Elimination Contract B. Personal communication with National Marine Fisheries Service (NMFS).

CALTRANS. 2009. *Technical guidance for assessment and mitigation of the hydroacoustic effects of pile driving on Fish.* Technical report prepared by ICF Jones & Stokes and Illingworth and Rodkin, Inc, for California Department of Transportation, Sacramento CA.

Carnes, M.R. 2009. Description and Evaluation of GDEM-V 3.0. NRL Memorandum Report 7330-09-9165. US Naval Research Laboratory, Stennis Space Center, MS. 21 p.

[CEDA] Central Dredging Association. 2011. *Underwater Sound in Relation to Dredging*. CEDA Position Paper–7. 6 p. http://www.dredging.org/documents/ceda/html_page/2011-11_ceda_positionpaper_underwatersound_v2.pdf

Collins, M.D. 1993. A split-step Pade solution for the parabolic equation method. *Journal of the Acoustical Society of America* 93(4):1736-1742.

Collins, M.D., R.J. Cederberg, D.B. King, and S.A. Chin-bing. 1996. Comparison of algorithms for solving parabolic wave equations. *Journal of the Acoustical Society of America* 100:178–182.

Coppens, A.B. 1981. Simple equations for the speed of sound in Neptunian waters. *Journal of the Acoustical Society of America* 69:862-863.

[CSA] Continental Shelf Associates Inc. 2004. *Explosive removal of offshore structures -information synthesis report*. OCS Study MMS 2003-070. U.S. Department of the Interior, Minerals Management Service, Gulf of Mexico OCS Region, New Orleans, LA. 181 p.

Dickerson, C., K.J. Reine, and D.G. Clarke. 2001. *Characterization of underwater sounds produced by bucket dredging operations*. DOER Technical Notes Collection (ERDC TN-DOER-E14), U.S. Army Engineer Research and Development Center, Vicksburg, MS. http://www.fakr.noaa.gov/protectedresources/whales/beluga/development/portofanc/erdc_dredge_noise_2001.pdf

Dzwilewski, P.T. and G. Fenton. 2003. *Shock wave/sound propagation modeling results for calculating marine protected species impact zones during explosive removal of offshore structures.* U.S. Dept. of the Interior, Minerals Management Service, Gulf of Mexico OCS Region, New Orleans, LA. OCS Study MMS 2003-059. 34 p. http://www.boem.gov/BOEM-Newsroom/Library/Publications/2003/2003-059.aspx

Ellis, D. and S. Hughes. 1989. *Estimates of sediment properties for ARPS*. DREA Memorandum TIAT-27. Defence Research Establishment Atlantic, Dartmouth, NS. 2 p.

Erbe, C. 2009. Underwater noise from pile driving in Moreton Bay, Qld. *Acoustics Australia* 37(3):87-92.

[FHWG] Fisheries Hydroacoustic Working Group. 2008. *Agreement in Principle for Interim Criteria for Injury to Fish from Pile Driving Activities. Memorandum*. http://www.wsdot.wa.gov/NR/rdonlyres/4019ED62-B403-489C-AF05-5F4713-D663C9/0/BA_InterimCriteriaAgree.pdf

Fisher, F.H. and V.P. Simmons. 1977. Sound absorption in sea water. *Journal of the Acoustical Society of America* 62(3):558-564.

Funk, D., D. Hannay, D. Ireland, R. Rodrigues, and W. Koski (eds.). 2008. *Marine Mammal Monitoring and Mitigation during Open Water Seismic Exploration by Shell Offshore Inc. in the Chukchi and Beaufort Seas, July–November 2007: 90-Day Report*. LGL Report P969-1. Prepared by LGL Alaska Research Associates Inc., LGL Ltd., and JASCO Research Ltd. for Shell Offshore Inc., National Marine Fisheries Service (US), and US Fish and Wildlife Service. 218 p. http://www-static.shell.com/static/usa/downloads/alaska/shell2007_90-d_final.pdf.

Gaboury, I., M. Zykov, S. Carr, and D. Hannay. 2007a. *Ladd deepwater marine coal terminal: assessment of underwater noise.* Technical report for DRven Corporation by JASCO Applied Sciences, 65 p.

Gaboury, I., R. Gaboury, and S. Carr. 2007b. *Downeast LNG import terminal: assessment of underwater noise impacts*. Technical report for Resource Systems Engineering Inc. by JASCO Research Ltd, 45 p.

Hamilton, E.L. 1980. Geoacoustic modeling of the sea floor. *Journal of the Acoustical Society of America* 68:1313-1340.

Hannay, D.E. and R.G. Racca. 2005. *Acoustic Model Validation*. Document 0000-S-90-04-T-7006-00-E, Revision 02. Technical report for Sakhalin Energy Investment Company Ltd. by JASCO Research Ltd. 34 p. http://www.sakhalinenergy.com/en/documents/doc_33_jasco.pdf

Hannay, D., A.O. MacGillivray, M. Laurinolli, and R. Racca. 2004. *Sakhalin Energy–Source Level Measurements from 2004 Acoustics Programme*. Report by JASCO Research Ltd., Victoria, BC.

Hyde, D. W. 1988. User's guide for microcomputer programs ConWep and FunPro applications of TM 5-855-1. "Fundamentals of protective design for conventional weapons".

Hyde, D. W. 1992. Conventional weapons effect computer program, US Waterways Experiment Station Instructional Report SL-88-1. U.S. Army Corps of Engineers.

Illingworth and Rodkin, Inc. 2007. *Compendium of Pile Driving Sound Data* (Appendix I). Prepared for The California Department of Transportation. 129 p. http://www.dot.ca.gov/hq/env/bio/files/pile_driving_snd_comp9_27_07.pdf

Ireland, D.S., R. Rodrigues, D. Funk, W. Koski, and D. Hannay. 2009. *Marine mammal monitoring and mitigation during open water seismic exploration by Shell Offshore Inc. in the Chukchi and Beaufort Seas, July–October 2008: 90-day report*. LGL Rep. P1049-1. Prepared by LGL Alaska Research Associates Inc., LGL Ltd., and JASCO Applied Sciences Ltd. for Shell Offshore Inc, Nat. Mar. Fish. Serv., and U.S. Fish and Wild. Serv. 277 p. plus appendices.

MacGillivray, A., G.R. Warner, R. Racca, and C. O'Neill. 2011. *Tappan Zee Bridge Construction Hydroacoustic Noise Modeling: Final Report.* Report by JASCO Applied Sciences for AECOM. 63 p. http://www.newnybridge.com/documents/feis/vol2/f-4a-tzb-construction-hydroacoustic-noise-modeling.pdf

Malme, C.I., P.R. Miles, G.W. Miller, W.J. Richardson, D.G. Roseneau, D.H. Thomson, and C.R. Greene Jr. 1989. *Analysis and ranking of the acoustic disturbance potential of petroleum industry activities and other sources of noise in the environment of marine mammals in Alaska.* BBN Systems and Technologies Corporation for Minerals Management Service U.S. Department of the Interior.

McGlaun, J.M., S.L. Thompson, and M.G. Elrick. 1990. CTH: A three-dimensional shock wave physics code. *International Journal of Impact Engineering* 10:351-360.

McHugh, O., M. Fraker, B. Wheeler, M. Austin, M. Zykov, and M. Laurinolli. 2007. *Potential Acoustic Impacts to Killer Whales Associated With Construction Dredging at DP3.* PROJECT NO. 1021281. Report prepared for Vancouver Port Authority by Jacques Whitford-AXYS and JASCO Research Ltd. 53 p.

Miles, P.R., C.I. Malme, and W.J. Richardson. 1987. *Prediction of Drilling Site-Specific Interaction of Industrial Acoustic Stimuli and Endangered Whales in the Alaskan Beaufort Sea*. OCS Study. MMS 87-0084. BBN Report No. 6509. Anchorage. AK: USDOI. MMS, Alaska OCS Region. 341 p.

Mosher, M. 1999. *Cape Fear River blasting mitigation test: Results of caged fish necropsies.* Final Report to CZR, Inc. under contract to U.S. Army Corps of Engineers, Wilmington District.

Mouy, X., and M. Zykov. 2009. *Underwater acoustic monitoring of pile driving activities in the Penobscot River, Bangor, Main*. Version 1.2, Technical report for RMT Inc. by JASCO Applied Sciences.

Nehls, G., K. Betke, S. Eckelmann, and M. Ros. 2007. *Assessment and costs of potential engineering solutions for the mitigation of the impacts of underwater noise arising from the construction of offshore windfarms*. Technical report for COWRIE by BioConsult SH.

Nützel, B. 2008. *Untersuchungen zum Schutz von Schweinswalen vor Schockwellen (Investigations to protect harbour porpoises from shock waves).* Technischer Bericht TB 2008–7, FWG. Kiel, Germany.

O'Neill, C., D. Leary, and A. McCrodan. 2010. Sound Source Verification. (Chapter 3) *In*: Blees, M.K., K.G. Hartin, D.S. Ireland, and D. Hannay (eds.). *Marine mammal monitoring and mitigation during open water seismic exploration by Statoil USA E&P Inc. in the Chukchi Sea, August-October 2010: 90-day report*. LGL Report P1119. Prepared by LGL Alaska Research Associates Inc., LGL Ltd., and JASCO Applied Sciences Ltd. for Statoil USA E&P Inc., National Marine Fisheries Service (US), and US Fish and Wildlife Service. pp. 3-1 to 3-34.

Porter, M.B. and Y.-C. Liu. 1994. Finite-element ray tracing. *In*: Lee, D. and M.H. Schultz (eds.). *Proceedings of the International Conference on Theoretical and Computational Acoustics*. Volume 2. World Scientific Publishing Co. pp 947-956.

Robinson, S.P., P.D. Theobald, G. Hayman, L.S. Wang, P.A. Lepper, V. Humphrey, and S. Mumford. 2011. *Measurement of noise arising from marine aggregate dredging operations.* MALSF. MEPF Ref no. 09/P108.

Rodriguez, E., C.S. Morris, Y.J.E. Belz, E.C. Chapin, J.M. Martin, W. Daffer, and S. Hensley. 2005. *An assessment of the SRTM topographic products.* JPL D-31639. Jet Propulsion Laboratory Pasadena, CA.

Southall, B.L., A.E. Bowles, W.T. Ellison, J.J. Finneran, R.L. Gentry, C.R. Greene Jr., D. Kastak, and D.R. Ketten. 2007. Marine mammal noise exposure criteria: Initial scientific recommendations. *Aquatic Mammals* 33(4):411–521.

Swisdak, Jr., M.M. 1978. *Explosion effects and properties: Part II - Explosion effects in water.* Naval Surface Weapons Center, Silver Spring, MD. NSWC/WOL TR 76-116. http://www.dtic.mil/cgi-bin/GetTRDoc?Location=U2&doc=GetTRDoc.pdf&AD=ADA056694

Teague, W.J., M.J. Carron, and P.J. Hogan. 1990. A comparison between the Generalized Digital Environmental Model and Levitus climatologies. *J. Geophys. Res.* 95(C5):7167-7183.

[USACE] U.S. Army Corps of Engineers, Waterways Experiment Station. 1999. Draft, Analysis of Water Shock Data and Bubble Screen Effectiveness on the Blast Effect Mitigation Test Series, Wilmington Harbor, NC. Vicksburg, MS. Prepared by Denis Rickman for U.S. Army Corps of Engineers, Wilmington District, Wilmington, NC.

Vagle, S. 2003. *On the impact of underwater pile-driving noise on marine life.* Technical report by Institute of Ocean Sciences, DFO/Pacific, Ocean Science and Productivity Division.

Warner, G., C. Erbe, and D. Hannay. 2010. Underwater sound measurements. (Chapter 3) *In*: Reiser, C.M., D.W. Funk, R. Rodrigues, and D. Hannay (eds.). *Marine Mammal Monitoring and Mitigation during Open Water Shallow Hazards and Site Clearance Surveys by Shell Offshore Inc. in the Alaskan Chukchi Sea, July-October 2009: 90-Day Report.* LGL Report P1112-1. Report by LGL Alaska Research Associates Inc. and JASCO Applied Sciences for Shell Offshore Inc., National Marine Fisheries Service (US), and US Fish and Wildlife Service. pp 3-1 to 3-54. http://www-static.shell.com/static/usa/downloads/alaska/report_2009_shell_90-d_report_plus_appendices.pdf.

Wright, D.G., and G.E. Hopky. 1998. Guidelines for the use of explosives in or near Canadian fisheries waters. Can. Tech. Rep. Fish. Aquat. Sci. 2107: iv + 34p. http://www.dfo-mpo.gc.ca/Library/232046.pdf

WSDOT. 2010a. *Underwater sound levels associated with driving steel piles for the State Route 520 bridge replacement and HOV project pile installation test program*. Technical report for Washington State Department of Transportation by Illingworth and Rodkin Inc.

WSDOT. 2010b. *Biological Assessment Preparation Advanced Training Manual*. Technical report by Washington State Department of Transportation.